Quaternary Science Reviews 301 (2023) 107936

Contents lists available at ScienceDirect

Quaternary Science Reviews

journal homepage: www.elsevier.com/locate/quascirev

Invited Review

The significance of volcanic ash in Greenland ice cores during the Common Era

Gill Plunkett [a, *], Michael Sigl [b], Joseph R. McConnell [c], Jonathan R. Pilcher [a], Nathan J. Chellman [c]

[a] Archaeology & Palaeoecology, School of Natural and Built Environment, Queen's University Belfast, Belfast, UK
[b] Climate and Environmental Physics & Oeschger Centre for Climate Change Research, University of Bern, Bern, Switzerland
[c] Desert Research Institute, Reno, USA

ARTICLE INFO

Article history:
Received 12 October 2022
Received in revised form
16 December 2022
Accepted 20 December 2022
Available online 10 January 2023

Handling Editor: Giovanni Zanchetta

Keywords:
Polar ice cores
Cryptotephra
Volcano-climate interactions
Volcanic ash dispersal
Late Holocene
Microparticles

ABSTRACT

Polar ice cores provide long, continuous and well-dated records of past volcanism and have contributed significantly to our understanding of volcanic impacts on climate and society. Sulphate aerosols deposited in the ice are essential for determining the effective radiative forcing potential of past eruptions, but calculations are improved with knowledge of eruption source parameters. Only the co-deposition of volcanic ash can presently confirm the source eruption. Here we review the current state of knowledge regarding the representation of volcanic ash in Common Era ice cores from Greenland and consider what the tephras reveal about the volcanic records in the ice. We augment the published record with a large dataset of previously unreported tephras, the result of a programme of targeted sampling guided by microparticle records that allow us to home in on tephra layers with variable temporal relationships to sulphate aerosol deposition. In addition to revealing the extensive source region of tephra that disperses to Greenland, our review explores for the first time some of the insights provided by the ash about the eruptions, such as the magma type and eruption style. We consider the characteristics of eruptions associated with varying degrees of climate responses and find that the strongest forcing tends to be associated with those producing mafic to intermediate tephra, and that phreatomagmatic processes are commonly involved. The frequent occurrence of multiple eruptions in these instances may also play a role in accentuating the climate response. We note consistencies in the timing of particulate and sulphate aerosol fallout from Icelandic (synchronous) and Alaskan (ash before sulphates) regions, with greater delays (one or more years) for stratospheric transport from tropical eruptions. We outline remaining avenues of research on ice-core tephra that promise to throw light on past volcanic eruption processes, including volatile release and transport, as well as the frequency and impact of small-to-moderate eruptions. We advocate greater integration of wide-ranging tephra research towards a better understanding of volcano-climate relationships.

1. Introduction

There is strong scientific consensus that volcanic eruptions impact hemispheric to global climate on annual to decadal timescales (Robock, 2000; Timmreck, 2012; Schurer et al., 2013; Sigl et al., 2015; Toohey et al., 2019). Traditionally, large magnitude, tropical eruptions have been regarded as the primary perpetrators of the most significant volcanically-forced climate anomalies in the past (e.g., Fischer et al., 2007; Swingedouw et al., 2017), and their greater forcing potential is supported by model simulations (Marshall et al., 2020). Yet increasingly the study of volcanic ash (fine-grained tephra) in polar ice cores is upturning these conventional views, highlighting a lack of simple correlation between climatically impactful eruptions and their source location, magnitude and style: the "large" (i.e., in terms of suspected climate impact) events include extra-tropical (Unknown 536 CE and Okmok 43 BCE; Sigl et al., 2015; McConnell et al., 2020) and fissure eruptions (Laki 1783 and Eldgjá 939; Fiacco et al., 1994; Zielinski et al., 1995). With tens of volcanic eruptions occurring every year (Siebert et al., 2010), what then determines whether an eruption will have a climate

* Corresponding author.
E-mail address: g.plunkett@qub.ac.uk (G. Plunkett).

https://doi.org/10.1016/j.quascirev.2022.107936

impact clearly outside the range of normal variability? Sulphur dioxide emissions, volcano latitude and season are the most important determinants of climate forcing potential (Toohey et al., 2016; Marshall et al., 2019), but there is now a greater effort to capture the role of photochemical speciation and aerosol evolution in controlling the extent and duration of chemical and radiative effects (LeGrande et al., 2016; Timmreck et al., 2018; Aubry et al., 2020), as well as the role of cloud responses (Gregory et al., 2016; Schmidt et al., 2018; Marshall et al., 2020; Chen et al., 2022). Remaining challenges include understanding initial chemical and physical conditions within the plume, including compound interaction with ash, and the role of atmosphere-ocean feedback (Kremser et al., 2016; Zanchettin et al., 2016). A recent inter-model comparison exercise highlighted the need for future models to attempt to consider the role of water and ash in the plume/cloud dynamics (Clyne et al., 2021). Ozone-destroying halogens co-emitted into the stratosphere have also been shown potentially to influence effective radiative forcing potential though there is limited agreement on the direction and strengths of these changes (e.g., Brenna et al., 2020; Staunton-Sykes et al., 2021). Notably, there has been greater recognition of the importance of recent small-to-moderate eruptions on both stratospheric and tropospheric processes (Gregory et al., 2016; Schmidt et al., 2018; Stocker et al., 2019; Staunton-Sykes et al., 2021), but their role in past climate forcing has not yet been investigated.

Greenland ice cores capture records of Northern Hemisphere and larger tropical eruptions, allowing their impacts to be considered within the context of long historical records and well-dated palaeoenvironmental proxies. Volcanic aerosols in the ice provide critical records of past volcanism but identifying the source eruptions – necessary for determining the extent of their atmospheric aerosol loading – can only be achieved through the geochemical characterisation of co-deposited volcanic ash (specifically, the glass component), if present in the ice. Extensive work has been conducted on Last Glacial ice, with volcanic ash highlighting the importance of Iceland as a source of volcanic fallout in Greenland through the last ice age (Davies et al., 2010, 2014; Abbott et al., 2012; Bourne et al., 2015; Cook et al., 2022). Tephra research on Holocene ice has been comparatively patchy, chiefly focusing on identifying the source of specific volcanic signals through geochemical matching of the ash, which has made important contributions to dating and synchronising ice cores (Grönvold et al., 1995; Coulter et al., 2012), and the recognition of volcanic impacts (e.g., Sigl et al., 2015; Büntgen et al., 2017; McConnell et al., 2020; Pearson et al., 2022). Here, we bring together previous research and a large dataset of newly identified tephras from the Common Era interval in Greenland ice cores to consider the state of the art in tephra research for this time period. We examine what can be gleaned from the existing data, and explore potential new avenues of research that may contribute to resolving some of the aforementioned uncertainties in volcano-climate modelling. To illustrate the great distances across which tephra is transported, Fig. 1 shows the locations of ice core drilling sites in Greenland at which Common Era tephra has been found, and the known or suspected sources of the tephra. We also consider the potential for intercontinental tephra-based correlations given the known distribution of Mid-to Late Holocene cryptotephra findspots in northeast America and northwest Europe. Ice cores and corresponding metadata, including relevant depth-age information, are summarised in Table S1.

2. Overview of research

2.1. Previously published tephras in Common Era Greenland ice cores

Abbott and Davies's (2012) review of Greenland tephra record reported eight tephra horizons, comprising 11 distinct geochemical populations, dating to the Common Era, including four of known (Icelandic) origin: Laki 1783 (Fiacco et al., 1994), Öraefajökull 1362 (Palais et al., 1991), Eldgjá 939 (933 GICC05 chronology; Zielinski et al., 1995) and the Settlement (or Landnám) Layer identified in both GRIP and GISP2 (Grönvold et al., 1995; Zielinski et al., 1997b). Amongst these tephras, a 1479 eruption of Mount St Helens, Washington, USA (Fiacco et al., 1993), and a 1259 eruption of El Chichón, Mexico (Palais et al., 1992), were proposed but the geochemical matches with these sources were unconvincing, reflecting to some extent methodological difficulties in obtaining accurate analyses from very small glass shards. De Silva and Zielinski (1998) recognised multiple eruptions contributing to potentially concurrent volcanic signals in ice cores from Antarctica (in which Huaynaputina tephra was identified) and Greenland (with tephra from an unidentified source) in the early 1600s. More compelling evidence for El Chichón tephra was identified by Zielinski et al. (1997a) from snow pits in central Greenland, in which minute (2–4 μm) glass shards with a major element geochemistry closely matching the 1982 eruptives were recovered. A second glass population was identified from larger (10–20 μm) shards and was surmised by Zielinski et al. (1997a) possibly to be from Bezymianny, Kamchatka, but a geochemical correlation to this source was not established.

Coulter et al. (2012) reported 11 further Common Era tephras, including – in NGRIP – Novarupta-Katmai 1912, and tephras subsequently correlated with the Millennium Eruption of Changbaishan, North Korea/China, in 946 (Sun et al., 2014; revised eruption date based on Oppenheimer et al., 2017), and Churchill, Alaska, eruption of 852/3 ± 1 (Jensen et al., 2014; revised date from Mackay et al., 2022). These tephras represented the first unambiguous identification of non-Icelandic tephra in Common Era Greenland ice along with geochemically confirmed tephra from the caldera-forming Aniakchak II eruption, Alaska, dated to 1628 or 1627 BCE (1641–39 BCE on the GICC05 chronology; Coulter et al., 2012; Plunkett et al., 2017; revised date from Pearson et al., 2022). The latter tephra had previously been identified in the GRIP ice core (Hammer et al., 2003) but its attribution had been debated (Pearce et al., 2004a; Vinther et al., 2008). Although not provenanced, the geochemistries of the many "unknown" tephras (i.e., of unknown source) were inconsistent with Icelandic material, and the seeming dominance of non-Icelandic tephras was noted by Coulter et al. (2012) to stand in contrast to Last Glacial and Early Holocene ice-core records in which the tephras were predominantly of Icelandic origin (Abbott and Davies, 2012). Diminutive shards (3–5 μm) with a geochemical composition approaching that of Vesuvius 79 tephra in GRIP (Barbante et al., 2013) provided further signs of an extensive source region for tephra reaching Greenland. The subsequent revision of the ice core chronology, moving the layer in question from 79 ± 0 to 88 ± 2 CE, and the recognition of a probable Alaskan tephra in NEEM-2011-S1 ice of the same age, later called this attribution into question (Plunkett et al., 2022). The c. 1259 GISP2 tephra analysed by Palais et al. (1992) was found to compare well on geochemical grounds to ash from the 1257 eruption of Samalas, Indonesia (Lavigne et al., 2013), marking the first possible record of a Southern Hemisphere tephra dispersing to Greenland. The GISP2 tephra analyses are characterised by wide standard deviations, however, and although they overlap with data from Samalas proximal material, further investigations of tephra from Greenland are needed to provide a robust correlation. More convincing data from Antarctica nevertheless confirm the association of the Samalas eruption with the major sulphate spike of 1259, as well as concurrent eruptions in Antarctica and possibly New Zealand (Narcisi et al., 2019). Independent confirmation that the sulphate deposited in Greenland

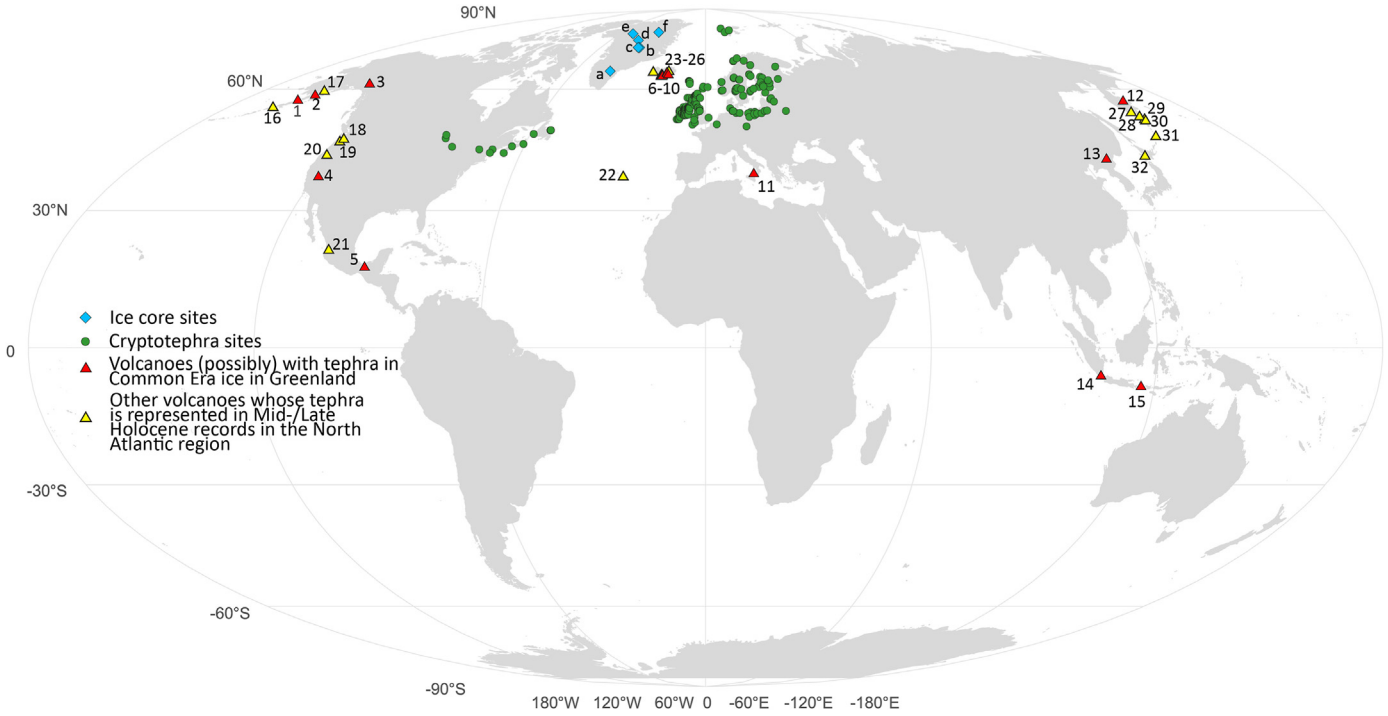

Fig. 1. Location of Greenland ice cores sites from which Common Era cryptotephra has been reported (a – Dye-3; b – GRIP; c – GISP2/Summit; d – NGRIP; e – NEEM; f – TUNU) and their (possible) sources (1 – Aniakchak; 2 – Novarupta-Katmai; 3- Churchill; 4 – Mono-Inyo Craters; 5 – El Chichón, 6–10 – Katla, Torfajökull, Veidivötn-Bárdarbunga, Grímsvötn, Öraefajökull; 11 – Lipari; 12 – Shiveluch; 13 – Changbaishan; 14 – Krakatau; 15 - Samalas). Also shown are the locations of Mid-to Late Holocene cryptotephra sites in northwest Europe and northeast America (Dörfler et al., 2012; Plunkett and Pilcher, 2018; Jones et al., 2020; Kalliokoski et al., 2019, 2020; Kinder et al., 2020, 2021; Vakhrameeva et al., 2020; Jensen et al., 2021; Martin-Puertas et al., 2021; Mackay et al., 2022), illustrating the present extent of cryptotephra records in the North Atlantic region. The (possible) sources of additional Mid-to Late Holocene cryptotephra found in the North Atlantic region are indicated to demonstrate the potential for inter-continental linkages (16 - Okmok; 17 – Augustine; 18 – Ranier; 19 - Mount St Helens; 20 – Mazama (Crater Lake); 21 – Ceboruco; 22 – Furnas; 23–26 – Snaefellsjökull, Hekla, Eyjafjallajökull, Askja; 27 – Khangar; 28 – Opala; 29 – Ksudach; 30 – Iliinsky; 31 – Ushishur; 32 – Tamurai).

and Antarctica around 1258–1260 is from the same source (Burke et al., 2019), or at least was formed and transported in the stratosphere (Baroni et al., 2008; Gautier et al., 2019), was provided by sulphur isotope measurements (Baroni et al., 2007).

With the analysis of the NEEM-2011-S1 and TUNU2013 ice cores, Late Holocene tephra investigations increased. The Millennium Eruption and Churchill tephras were identified in NEEM-2011-S1, providing accurate tie-points with NGRIP (Jensen et al., 2014; Sun et al., 2014). Tephra from a second source, possibly in Japan, was recorded amongst Millennium Eruption glass in the NEEM-2011-S1 sample (Sun et al., 2014; Plunkett et al., 2017). Sun et al. (2014) also examined ice spanning the Eldgjá 939 eruption and found only two shards with disparate geochemical compositions, neither of which matched Eldgjá. Sigl et al. (2015) reported the presence of tephra associated with a large sulphate event at 536 in NEEM-2011-S1 which has been linked to a pronounced climate anomaly in the Northern Hemisphere (Toohey et al., 2016; van Dijk et al., 2022). The geochemistry of the glass, comprising multiple distinct populations, suggests that the ash derives from at least three different sources, implying coeval eruptions. Although none of the glass populations could be firmly attributed to a source, the geochemical compositions are consistent with mid-to high latitude volcanic regions (including Aniakchak and Mono-Inyo Craters) but distinctive from Iceland.

Sun et al.'s (2014) investigation of the Millennium Eruption was the first study to identify co-registered non-sea salt sulphur and microparticle peaks as a diagnostic tracer for the presence of cryptotephra in ice cores. Since then, six more volcanic eruptions have been identified in polar ice cores on the basis of this association, further validating the effectiveness of this approach (Jensen et al., 2014; McConnell et al., 2017, 2020; Dunbar et al., 2017; Abbott et al., 2021; Smith et al., 2020). For comparison, without such criteria, Coulter et al. (2012) had analysed as much as 93 m of Late Holocene ice cores (695 discrete samples) to detect as few as 17 samples containing tephra. The relationship between microparticles and tephra is further emphasised by a quasi-annual analysis of two 20-year-long periods (815–835 CE) of ice in the NEEM-2011-S1 and TUNU2013 cores that found tephra presence to correlate with increased levels of microparticles (Plunkett et al., 2020). The study found tephra in low concentrations in six of the 43 samples, of which only one (correlating to Katla, Iceland) could be firmly tied to a source eruption dated to between 822 and 823 using dendrochronology (Büntgen et al., 2017).

The continuous microparticle record from TUNU2013 prompted a targeted sampling strategy, reported here for the first time, that focused precisely on notable microparticle peaks, with samples immediately above and below the peak (dubbed "buffers") as a control on the relationship of microparticles and larger ash shards. Events were selected either to 1) replicate previous results and provide tie-points with other cores, 2) identify the source of prominent sulphate or microparticle spikes, or 3) establish precise dates for suspected eruptions. Samples were cut in the Desert Research Institute, Reno, and shipped to Belfast for examination, mounting and major element geochemical characterisation (see SI for methods and Supplementary Dataset 1 for analytical conditions). Of the 16 events, 15 were found to be associated with at least one shard of tephra, and tephra was also present in five of the buffer samples, although some of these buffers also featured minor increases in microparticles (Fig. 2). Only the 1606 target had no certain tephra, but in some instances (1810, 1478/9 and 649/50),

small shard size (<20 μm) and/or the presence of microlite crystals in the glass impeded successful geochemical analysis. The results of two targets have already been reported: Ilopango, El Salvador, tephra was identified at 431 ± 2, resolving a much-debated question regarding the age of the Tierra Joven Bianca ash (Smith et al., 2020), and an acid signal at 1477 was confirmed as deriving from Veidivötn-Bárdarbunga (Abbott et al., 2021). The results of major element geochemical characterisation of the remaining investigations are outlined in Section 2.2. We also examined a series of sub-annual samples bracketing ice dating to 1104 to test for the presence of Hekla 1104 tephra. Additionally, we report here previously unpublished tephras from the NEEM-2011-S1 ice core. These samples were cut with respect to specific events in the sulphate record. The glass characterisation of all new tephras is shown in Fig. 3. A summary of all tephras found in Common Era Greenland ice cores is presented in Table 1. The major element geochemistry of the newly reported tephras, and microscope images of the shards, are provided in the Supplementary Datasets 1 and 2, respectively. Table S1 summarises the Greenland Mid-to Late Holocene tephra record, including updated age estimates for pre-historic tephras.

2.2. TUNU2013 – previously unpublished tephras

2.2.1. 1989 ± 3 Unknown

A prominent microparticle peak (maximum 0.7 μg/g) in approximately 1989 was examined to determine the potential source of a synchronous and significant nssS spike (Fig. 2A). Three small (<20 μm) but blocky colourless particles were identified as possible tephra (QUB-1943). Analysis was possible on one shard only, which has a rhyolitic composition. Successive analyses produced heterogenous results, however, notably in Al and Na concentrations, although there were no obvious microlites present in the glass to explain the variability. The origin of this shard has not been determined but it has significantly higher MgO and lower Ca and K content than tephra from Redoubt, Alaska (Cameron et al., 2019), ruling out any link to the 1989 eruption.

2.2.2. 1884 ± 1 Unknown, 1885 ± 1 Unknown

The 1883 Krakatau eruption, Indonesia, has been estimated to have had a cumulative radiative forcing potential of −5.5 W m^{-2} on the basis of sulphate signals in bipolar ice cores (Sigl et al., 2015). It has been credited as an inspiration for a series of paintings by American and European artists in the years that followed (Zerefos et al., 2007). In the same year, however, a large (VEI 4) eruption of Augustine, as well as small-to-moderate (VEI 2 or 3) eruptions of four other Aleutian volcanoes, may have contributed to the optical effects observed in the Northern Hemisphere. In the TUNU2013 core, we targeted a moderate spike in microparticles in 1885, capturing a smaller spike in the underlying buffer sample dating to 1884 (Fig. 2B). The lower microparticle spike slightly lags a small increase in nssS, while the 1885 peak is coeval with a larger sulphur rise.

The lower buffer (QUB-1945) yielded a single brown, cuspate shard (40 μm) with microlites, from which four analyses indicate an andesitic composition. The main sample (QUB-1944) contained a microlitic brown tephra shard (30 μm) and a colourless shard (40 μm), from which seven and three replicated analyses were obtained, respectively. The colourless shard has a rhyodacitic composition, while the brown shard is tephriphonolitic, with a notably high P content. The compositions of the QUB-1945 shard

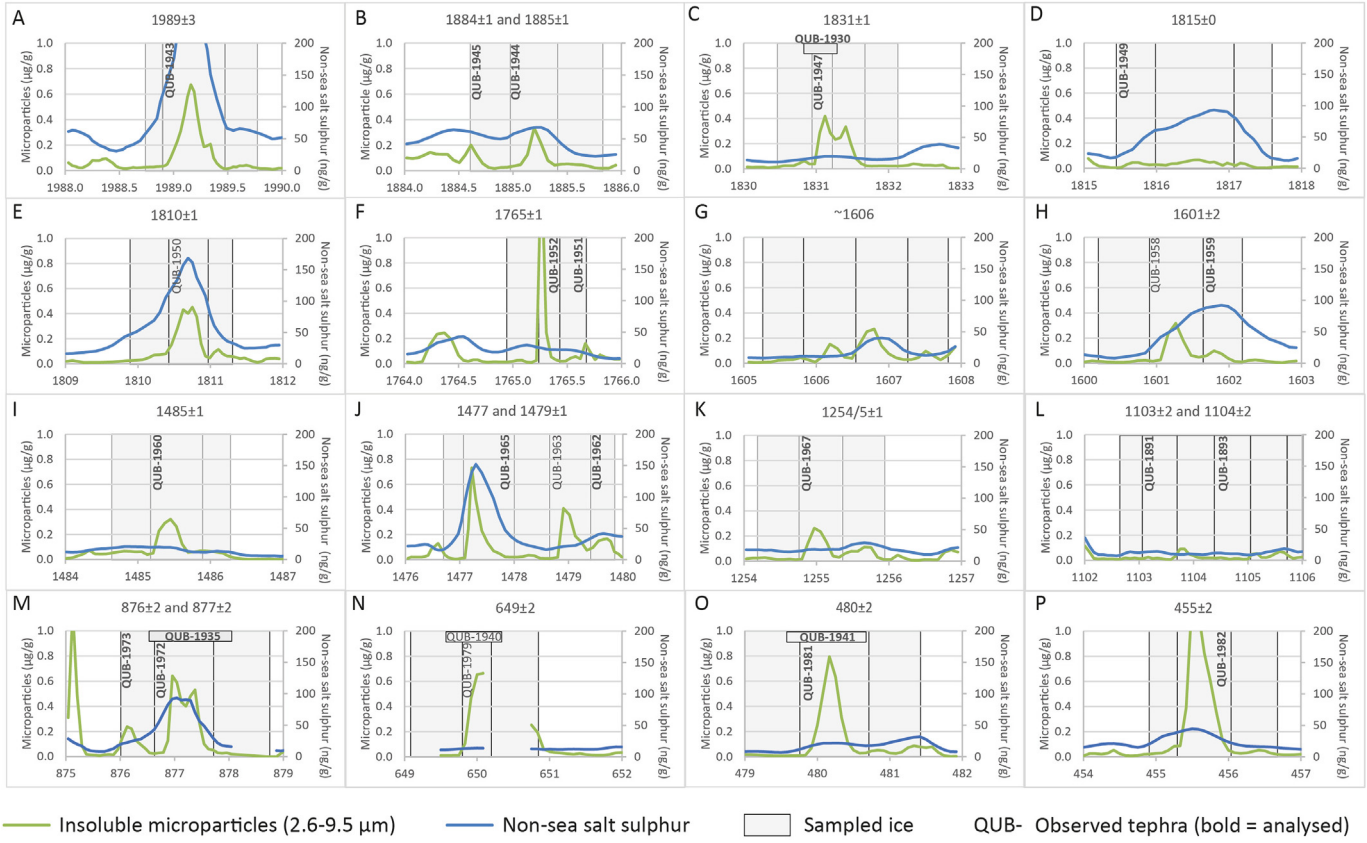

Fig. 2. The positions of tephra samples from the TUNU2013 ice core, shown with respect to microparticle and non-sea salt sulphur data from the TUNUredo analysis. QUB- codes indicate the samples found to contain tephra shards, with bold type indicating tephras that were analysed for major element geochemistry. For inter-core comparisons, see Fig. S1.

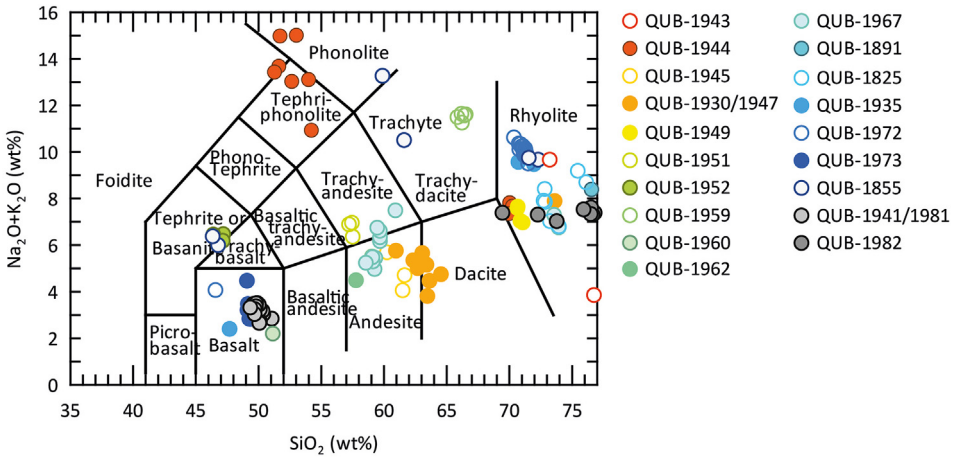

Fig. 3. Total alkali silica plot (following Le Bas et al., 1986) showing glass compositions of tephras reported in this paper. A symbol-based version of this plot is presented in the Supplementary Information (Fig. S1).

and the colourless shard in QUB-1944 are similar to glass from Krakatau 1883 but also sit within the range of many products from Alaskan/Aleutian sources, although not specifically with Augustine tephra (Fig. 4). Alaskan tephra is most likely deposited in Greenland within weeks of an eruption (Plunkett et al., 2022). The timing of the tephra in TUNU2013 would therefore appear to be late for any material from an 1883 eruption in that region. Tephra from the 1991 eruption of Pinatubo was deposited in Antarctica in 1993 and 1994 (Cole-Dai et al., 1997), highlighting the potentially greater delay of ash arriving from the tropics. It is possible, therefore, that the TUNU2013 ash derives from stratospheric transport of Krakatau tephra, but trace element analysis of the tephra is required to differentiate robustly its source(s). The origin of the tephriphonolitic shard has not been established.

2.2.3. 1831 ± 1 Kuriles

Multiple samples were extracted to identify the source of a sulphate peak previously attributed to Babuyan Claro, Philippines (Zielinski, 1995). Recently, Garrison et al. (2021) argued that the sulphate derives from Ferdinandea, Italy, the date of the Babuyan Claro eruption having been discredited (Garrison et al., 2018). Tephra was identified in two overlapping samples (QUB-1930: 92 shards; QUB-1947: 75 shards) that centred on the microparticle peak dating to early 1831 (Fig. 2C). Both samples contained high concentrations of platy to cuspate, pale brown tephra shards, most of which were extremely fine-grained (~10 μm) with frequent microlites that impeded geochemical analysis. Altogether, 16 analyses were obtained, mainly low K andesitic to dacitic in composition with a single rhyolitic outlier (labelled QUB-1930/47). The geochemistry points to a source in the Kurile Islands (T. Hasegawa, pers. comm., March 2022; Fig. 5A); work is ongoing to confirm the exact provenance. No tephra was found associated with the secondary particle peak. The delay between the particles and the sulphur is greater than what would be expected for an eruption in the Kuriles, which implies that a second eruption, perhaps Ferdinandea, was responsible for the sulphate peak.

2.2.4. 1815 Unknown

The 1816 sulphate peak that has been attributed to the 1815 eruption of Tambora, Indonesia, is synchronous with a muted peak in microparticles (Fig. 2D). No tephra was found in the 1816 ice, but the lower buffer (QUB-1949), dating to 1815, yielded a single colourless, blocky large (44 μm) shard, from which multiple analyses were obtained. The rhyolitic geochemistry matches the low Si rhyolitic component of BTD-15 (~1650–1750 CE) and two older cryptotephras in northwest Europe (see Plunkett and Pilcher, 2018, Fig. 6A). The source of the tephra is uncertain. Plunkett and Pilcher (2018) surmised a possible Katla origin for the European cryptotephras on the basis of their recurrent association with ash matching silicic Katla eruptives but there is no reported eruption of this volcano in 1815.

2.2.5. 1810 ± 1 Unknown

A prominent sulphate spike at 1809/1810 in polar ice cores attributed to a possible tropical eruption has been linked to significant global climate impacts (Cole-Dai et al., 2009; Timmreck et al., 2021). Tephra reported from Antarctica and the Eclipse Ice field, Canada, indicate multiple eruptions around this time (de Angelis et al., 1985; Palais et al., 1990; Kurbatov et al., 2006; Yalcin et al., 2006). The Siple Dome tephra derives from a probable Antarctic source (Kurbatov et al., 2006), and the Eclipse tephra falls within the compositional range of Alaskan eruptives (Yalcin et al., 2006), indicating coincidental eruptions in the higher latitudes. Notwithstanding some slight differences in geochemistry that may be due to instrumental error, the Dome C (de Angelis et al., 1985) and South Pole (Palais et al., 1990) tephras seem similar to each other, and are comparable to Indonesian tephra (e.g., Telaga Group F tephra reported by Faral et al., 2022). A combination of tropical and extra-tropical eruptions occurring in short succession may therefore have contributed to the climate response at this time.

In TUNU 2013, the 1810 sulphate spike is coeval with a prominent particle spike (Fig. 2E). This level yielded three small (8–15 μm), brown, microlitic tephra shards that were unsuitable for geochemical analysis (QUB-1950). Our findings nevertheless demonstrate potential for future studies to isolate tephra associated with this event.

2.2.6. 1765 ± 1 Unknown (North Atlantic?), 1765 ± 1 Unknown

A prominent microparticle peak dating to 1765 sits between sulphate peaks dating to 1764 and 1767. Individual brown tephra shards were found in samples corresponding to the particle peak and the ice immediately above (Fig. 2F). Analyses were obtained on two of these shards. The lower tephra (QUB-1952), coincident with the microparticle peak, comprised a single blocky to cuspate shard with a high phosphorus trachy-basaltic composition character. The geochemical composition bears some similarity to material from Jan Mayen (Gjerløw et al., 2015) but QUB-1952 has a much higher P content (Fig. 7). A similarly high P content can be found in tephra

Table 1
Common Era tephras reported from Greenland ice cores.

NS1-2011 Age	Source	Ice Core	Depth (m) from	Depth (m) to	Reported Age (CE)	Code	Glass geochemistry	Method	Reference
1989	Unknown	TUNU2013	7.40	7.22		QUB-1943	Rhyolitic	SEM-EDS/WDS	this paper
1983	El Chichón	Summit Pit 90-1	5.00	4.95	1983	Glass A	Rhyolitic	AASEM/EDS	Zielinski et al. (1997a)
	Unknown					Glass B	Rhyolitic		
1912	Novarupta-Katmai	NGRIP	28.45	28.25	1912	QUB-1004	Rhyolitic	EPMA	Coulter et al. (2012)
1885	Unknown	TUNU2013	27.93	27.85		QUB-1944	Rhyodacitic/tephriphonolitic	SEM-EDS/WDS	this paper
1884	Unknown	TUNU2013	27.99	27.93		QUB-1945	Andesitic	SEM-EDS/WDS	this paper
1831	Kuriles	TUNU2013	36.50	36.45		QUB-1930/47	Andesitic to dacitic	SEM-EDS/WDS	this paper
1815	Unknown (Katla?)	TUNU2013	38.97	38.91		QUB-1949	Rhyolitic	SEM-EDS/WDS	this paper
1810	Unknown	TUNU2013	39.68	39.60		QUB-1950		not analysed	this paper
1783	Unknown	GISP2-B	~71.4		1783	Glass B	Andesitic to dacitic	AASEM/EDS	Zielinski et al. (1994)
	Laki (Grímsvötn)	GISP2-B	71.34	71.30	1783	Glass C	Basaltic	AASEM/EDS	Fiacco et al. (1994); Zielinski et al. (1994)
1784	Unknown	GISP2-B	~71.3		1784	Glass A	Andesitic to dacitic	AASEM/EDS	Zielinski et al. (1994)
1765	Unknown (N. Atlantic?)	TUNU2013	45.97	45.91		QUB-1951	Trachy-andesitic	SEM-EDS/WDS	this paper
1765	Unknown	TUNU2013	46.02	45.97		QUB-1952	Trachy-basaltic	SEM-EDS/WDS	this paper
1601	Unknown	GISP2	117.30		1604		Trachy-andesitic?	AASEM/EDS	de Silva and Zielinski (1998)
1601	Unknown (Changbai?)	TUNU2013	64.88	64.82		QUB-1959	Trachytic	SEM-EDS/WDS	this paper
1485	Veidivötn-Bárdarbunga	TUNU2013	77.63	77.55		QUB-1960	Basaltic	SEM-EDS/WDS	this paper
1479	Unknown	TUNU2013	78.38	78.32		QUB-1962	Andesitic	SEM-EDS/WDS	this paper
1479	Unknown	TUNU2013	78.45	78.38		QUB-1963	Andesitic and dacitic	SEM-EDS/WDS	this paper
1477	Unknown	GISP2	147.30	1427.30	1479		Rhyolitic	AASEM/EDS	Fiacco et al. (1993)
1477	Veidivötn-Bárdarbunga	TUNU2013	78.61	78.50	1478	QUB-1965	Basaltic	SEM-EDS/WDS	Abbott et al. (2021)
1364	Unknown	Dye-3	326.15	325.80	1364	QUB-1303/4	Rhyolitic	EPMA	Coulter et al. (2012)
1362	Öraefajökull	GISP2	174.10		1362		Rhyolitic	AASEM/EDS	Palais et al. (1991)
		GRIP	165.40	165.20	1362	QUB-1052	Rhyolitic	EPMA	Coulter et al. (2012)
1259	Samalas?	GISP2	200.08	199.47	1259		Rhyodacitic	AASEM/EDS	Palais et al. (1992)
1254	Lipari?	NGRIP	162.65	162.45	1254	QUB-1360	Rhyolitic	EPMA	Coulter et al. (2012)
1254/5	Unknown (Iceland?)	TUNU2013	103.78	103.71		QUB-1967	Andesitic	SEM-EDS/WDS	this paper
1104	Unknown	TUNU2013	120.99	121.09		QUB-1893	Rhyolitic	SEM-EDS/WDS	this paper
1104	Unknown	NGRIP	190.15	189.95	1101	QUB-1186	Rhyolitic	SEM-EDS/WDS	Coulter et al. (2012)
1103	Unknown	TUNU2013	121.29	121.19		QUB-1891	Rhyolitic	SEM-EDS/WDS	this paper
959/60	Mono Craters?	NGRIP	216.35	216.15	953–4	QUB-1425	Rhyolitic	SEM-EDS/WDS	Coulter et al. (2012)
946/7	Changbaishan	NGRIP	218.55	218.35	941–2	QUB-1437	Trachytic/rhyolitic	SEM-EDS/WDS	Coulter et al. (2012)
		NEEM-2011-S1	247.13	247.29	941–2	QUB-1819 a & b	Trachytic/rhyolitic	SEM-EDS/WDS	Sun et al. (2014)
	Unknown (Japan?)	NEEM-2011-S1	247.13	247.29	941–2	QUB-1819c	Rhyolitic	SEM-EDS/WDS	Sun et al. (2014); Plunkett et al. (2017)
939	Eldgjá (Katla)	GISP2	274.40	272.20	938 ± 4	Glass A	Basaltic-andesitic	AASEM/EDS	Zielinski et al. (1995)
	Eldgjá?	GISP2	274.40	272.20	938 ± 4	Glass B	Dacitic	AASEM/EDS	Zielinski et al. (1995)
940	Unknown	NEEM-2011-S1	248.53	248.70	934	QUB-1823	Rhyolitic	SEM-EDS/WDS	Sun et al. (2014)
938	Unknown	Dye-3	494.85	494.45	931	QUB-1212/3	Rhyolitic	EPMA	Coulter et al. (2012)
914	Unknown	NGRIP	224.60	224.40	907–8	QUB-1470	Trachydacitic	SEM-EDS/WDS	Coulter et al. (2012)
881	Unknown (Kamchatka?)	NEEM-2011-S1	260.79	260.14		QUB-1825	Rhyolitic	SEM-EDS/WDS	this paper
877	Settlement	GISP2	286.40	286.25	877 ± 4		Basaltic/rhyolitic	AASEM/EDS	Zielinski et al. (1997b)
		GRIP	269.50	269.22	871 ± 1		Basaltic/rhyolitic	EDS	Grönvold et al. (1995)
		TUNU2013	146.49	146.37		QUB-1935	Basaltic/rhyolitic	SEM-EDS/WDS	this paper
877	Settlement: Torfajökull	TUNU2013	146.48	146.40		QUB-1972	Rhyolitic	SEM-EDS/WDS	this paper
876	Settlement: Veidivötn-Bárdarbunga	TUNU2013	146.54	146.48		QUB-1973	Basaltic	SEM-EDS/WDS	this paper
852/3	Churchill	NGRIP	235.25	235.05	846–7	QUB-1528	Rhyolitic	SEM-EDS/WDS	Coulter et al. (2012)
		NEEM-2011-S1	265.13	266.65	846–7	QUB-1830	Rhyolitic	SEM-EDS/WDS	Jensen et al. (2014)
824	Unknown (Mexico?)	TUNU2013	151.71	151.61		QUB-1880	Rhyolitic	SEM-EDS/WDS	Plunkett et al. (2020)
822	Katla	TUNU2013	152.39	152.30		QUB-1974	Basaltic	SEM-EDS/WDS	Plunkett et al. (2020)
817	Unknown (Alaska?)	TUNU2013	152.41	152.31		QUB-1873	Trachydacitic	SEM-EDS/WDS	Plunkett et al. (2020)
816	Unknown (N. Pacific?)	TUNU2013	152.51	152.41		QUB-1872	Rhyolitic	SEM-EDS/WDS	Plunkett et al. (2020)
815	Unknown	NEEM-2011-S1	273.35	273.13		QUB-1835	Rhyolitic	SEM-EDS/WDS	Plunkett et al. (2020)
649/50	Unknown	TUNU2013	171.04	170.98		QUB-1940		not analysed	this paper
536	Unknown, multiple	NEEM-2011-S1	327.25	327.17	530	QUB-1859	Mixed	SEM-EDS/WDS	Sigl et al. (2015)
531	Inyo Craters? Unknown	NEEM-2011-S1	328.06	327.84		QUB-1855	Mixed	SEM-EDS/WDS	this paper

480	Veidivötn-Bárdarbunga	TUNU2013	188.71	188.63		QUB-1941/81	Basaltic	SEM-EDS/WDS	this paper
455	Shiveluch?	TUNU2013	191.24	191.16		QUB-1982	Rhyolitic	SEM-EDS/WDS	this paper
431	Ilopango	TUNU2013	194.08	193.96		QUB-1983	Rhyolitic	SEM-EDS/WDS	Smith et al. (2020)
93–95	Unknown	NGRIP	366.85	366.70	85–87	QUB-1328	Basaltic	EPMA	Coulter et al. (2012)
88	Unknown (Alaska?)	NEEM-2011-S1	410.85	410.40		QUB-1832/3	Andesitic	SEM-EDS/WDS	Plunkett et al. (2022)
88	Vesuvius?	GRIP	429.30		79		Phonolitic	SEM-EDS	Barbante et al. (2013)

from the Canary Islands, but insufficient reference data from this region exist for a reliable comparison. The overlying sample (QUB-1951) captures the start of a minor increase in microparticles and produced a trachy-andesitic shard with a distinctive high K calc-alkaline composition (Fig. 7). Its source could not be determined.

2.2.7. 1601 ± 2 Unknown (Changbai?)

The 1601 bipolar sulphate peak linked by tephra in Antarctic ice to the eruption of Huaynaputina (de Silva and Zielinski, 1998) is associated in TUNU2013 with a moderate microparticle spike (Fig. 2H). Two small brown tephra shards (~20 μm) were found at the level of the microparticle peak (QUB-1958), but contained too many microlites to be suitable for glass analysis. A very large brown shard (150 μm) was found in the sample corresponding to the peak in nssS (QUB-1959). Its major element geochemistry is distinct from that of Huaynaputina and the 1601 GISP2 glass (de Silva and Zielinski, 1998), but matches the trachytic end-member of Changbaishan tephras (Sun et al., 2014, 2018). The only eruption posited from the Changbai system at this time is possibly that of the Wangtian'e cone in August 1597 (Li, 2013). No geochemical data for tephra from this event have been found for comparison, but the eruption is considered to have been only moderately explosive. It is difficult to reconcile such a modest eruption with the transport of a coarse shard to Greenland several years later, but given the strong geochemical correlation with Changbaishan tephra, this system seems at present to be the most likely source of the QUB-1959 tephra.

2.2.8. 1485 ± 1 Veidivötn-Bárdarbunga

A notable peak in microparticles at 1485 occurs in the absence of any change in nssS (Fig. 2.I). The event was sampled to establish if it derived from Mount St Helens eruptions whose tephra has been identified in northeast America and possibly Ireland (Mackay et al., 2016; Plunkett and Pilcher, 2018; Jensen et al., 2021). The sample contained one brown, cuspate shard (QUB-1960). The chemistry is consistent with Veidivötn-Bárdarbunga. While the shard and microparticles might signify remobilisation of ash from the large 1477 eruption of Veidivötn-Bárdarbunga in Iceland, the glass shows no sign of chemical or physical weathering. Haflidason et al. (2000) report a Veidivötn-Bárdarbunga tephra immediately above the 1477 tephra, which they date to ~1480, indicating a second eruption in this timeframe.

2.2.9. 1479 ± 1 Unknown

A significant microparticle peak at 1477 was targeted as a suspected link, subsequently confirmed, to the February 1477 eruption of Veidivötn (Abbott et al., 2021). Secondary particle peaks at 1479 coincided with elevated nssS (Fig. 2J). The larger peak (QUB-1963) contained at least seven small, brown, microlitic shards that were generally unsuitable for geochemical glass analysis. Analyses from two shards yielded poor results, yet indicated dissimilar glass compositions; one dacitic shard gave a poor analytic total (<90 wt %), while the second shard is andesitic but with elevated Al and Ca that imply entrapment of a plagioclase microlite. The overlying sample (QUB-1962) yielded a single platy, brown shard (25 μm). Only one analysis was obtained from the shard, indicating an andesitic composition. We find no geochemical match for the glass.

2.2.10. 1254/5 ± 1 Unknown

A moderate peak in larger microparticles at 1254/5 was investigated as previous research had located tephra with a geochemistry resembling that of Lipari (Italy) glass in the NGRIP core (Coulter et al., 2012; Plunkett and Pilcher, 2018, Fig. 2K). A mix of predominantly brown, small, platy shards (n. ≥26) was found in the sample corresponding to the particle peak (QUB-1967). Small shard

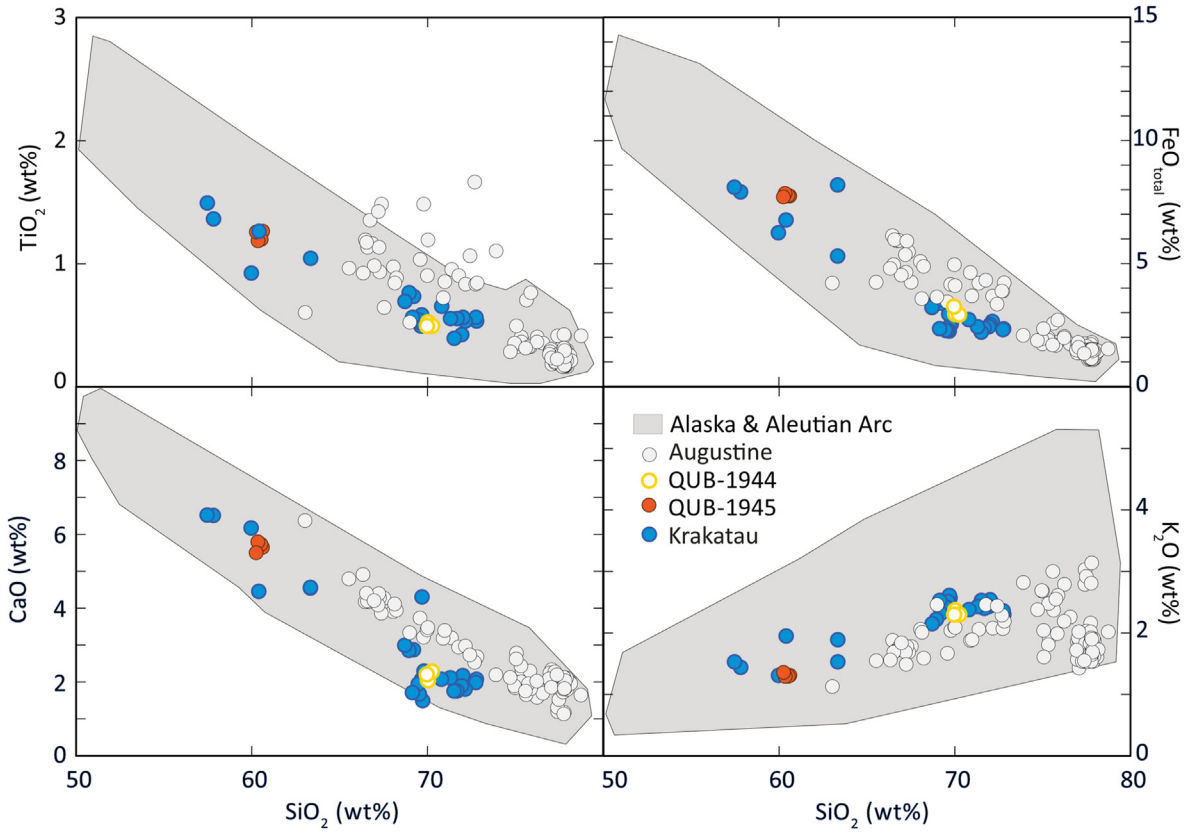

Fig. 4. Major element glass geochemistry of QUB-1944 and -1945 compared to tephra from Krakatau 1883 (Mandeville et al., 1996) and data from the Alaskan and Aleutian Arc that lie within the geochemical range of the ice core tephras (Cameron et al., 2019). Augustine tephra is shown for comparison (Larsen et al., 2010; Cameron et al., 2019).

size (mainly <30 μm) and the presence of microlites hindered analysis and resulted in low analytical totals or aberrant results. Thirteen shards returned a homogenous geochemical composition, indicating an andesitic glass similar to Katla and Hekla (Iceland) intermediate tephra (Fig. 6B). Possible Katla tephra has been identified in Ireland and Norway around this time (Plunkett and Pilcher, 2018) but neither volcano is known to have erupted in this interval. One shard has a geochemistry consistent with Churchill (Alaska) tephra. There is also no Churchill eruption known from this time period, although Churchill-type tephra has been recorded as a cryptotephra in Irish peatlands dating to around 1100 CE (Plunkett and Pilcher, 2018).

2.2.11. 1103 ± 2 Unknown, 1104 ± 2 Unknown

The interval between 1102 and 1106 was examined in an attempt to locate tephra from the 1104 eruption of Hekla, a key marker used in the GICC05 ice core chronology (Vinther et al., 2006). Coulter et al. (2012) had previously investigated this time-frame in NGRIP, and had recorded a tephra of uncertain origin (QUB-1186; then dated at 1101, and recently revised to 1104 ± 3; Sinnl et al., 2022), immediately following a small peak in electrical conductivity. In TUNU 2013, we found tephra particles in ice dating to 1104 ± 2 (QUB-1893) and 1103 ± 2 (QUB-1891), each sample corresponding to a small increase in sulphur and microparticles in the ice (Fig. 2L). QUB-1893 comprised a single shard (colourless, fluted, 50 μm along its long axis), from which three analyses were obtained. The results indicate a high Si/low Fe rhyolite, but the poor quality of the results (low totals, heterogeneity when normalised) calls into question their robustness. Other possible shards were found to be plagioclase. QUB-1891 contained similar particles to QUB-1893, but only one (a colourless, blocky shard, 50 μm along its long axis) returned a composition consistent with volcanic glass. Its geochemistry is similar to, but slightly more evolved than, that of QUB-1186. Comparable material has been identified in older Greenland ice at 946, 939 and 536 in very low concentrations (typically 1–2 shards) amongst various other tephras (Sun et al., 2014; Sigl et al., 2015). Geochemically similar tephra dating to within the last two centuries has also been reported by Jensen et al. (2021) from Sidney Bog, Maine (USA). Difficulties resolving the sources of these tephras are discussed further in Section 3.1. The eruptions associated with the QUB-1893 and -1891 tephras are precursors to the event responsible for a prominent sulphate peak beginning in 1108 which has been linked to climate anomalies and tentatively attributed to an eruption of Mt. Asama, Japan in 1108, and further eruptions in the lower and northern latitudes at about the same time (Guillet et al., 2020).

2.2.12. 877 ± 2 Settlement tephra (Vatnaöldur/Torfajökull)

The 877 sulphate spike, previously correlated in GISP2 and GRIP ice cores to the Icelandic Settlement (or Landnám) tephra (Grönvold et al., 1995; Zielinski et al., 1997b), was sampled to establish a robust tie-point between ice cores. The Settlement tephra was produced by simultaneous and interlinked eruptions of Vatnaöldur (part of the Bárdarbunga volcanic system) and Torfajökull in southern Iceland (Larsen, 1984). The former dispersed ash in all directions around the volcano, but Torfajökull tephra fell mainly to the west and northwest of the vent (Larsen, 1984; Thordarson and Höskuldsson, 2008). Although the Torfajökull eruption was likely triggered by initial activity in the Bárdarbunga system (Blake, 1984), in areas where both components were

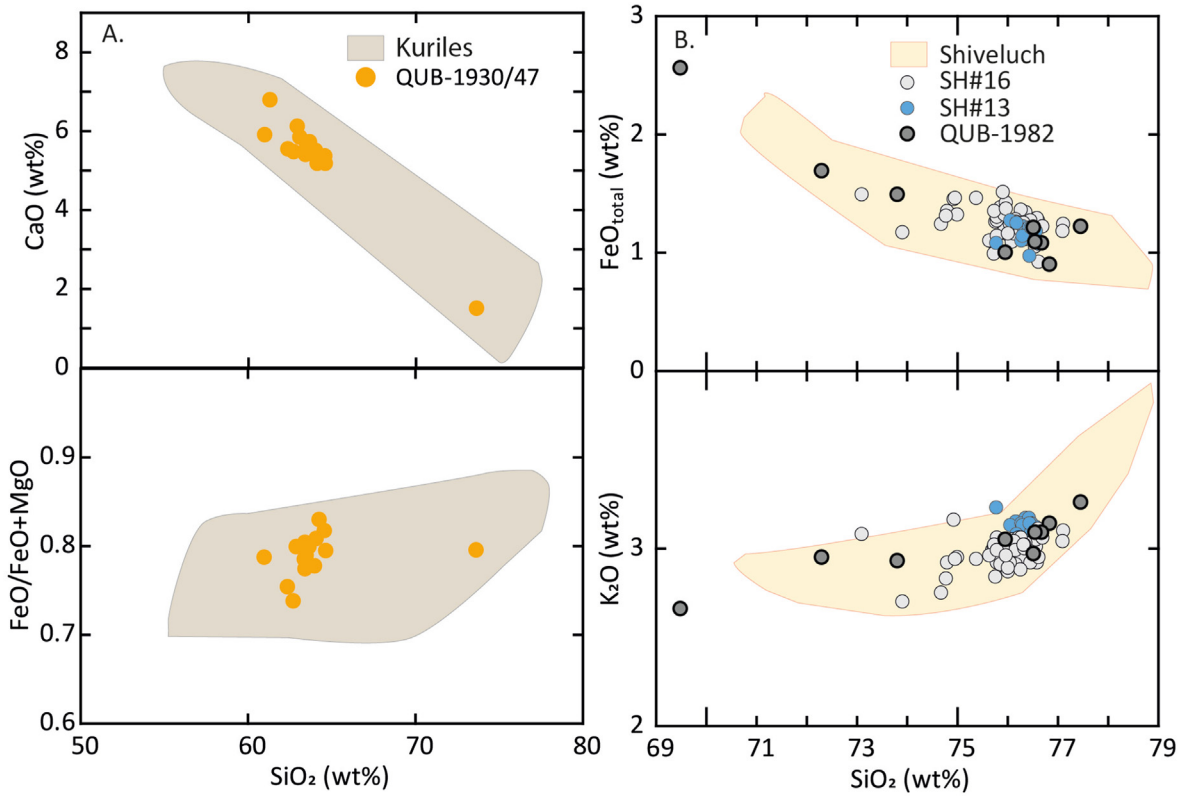

Fig. 5. Major element glass geochemistry of tephra sourced to Kamchatka and the Kurile Islands. (A) QUB-1930/47 compared to the compositional field of tephra from the Kurile Islands (based on Hasegawa et al. (2011) and Plunkett et al. (2022). (B) QUB-1982 plotted against the rhyodacitic-rhyolitic tephra from first millennium CE eruptions of Shiveluch (Ponomareva et al., 2015). QUB-1982 most closely matches unit SH#18 (~400 CE) and SH#13 (~500 CE) but its wider compositional range favours the former as a correlative.

deposited, visible beds comprise a twin-coloured layer typically featuring a lowermost white (silicic) unit of Torfajökull ash, topped by an olive-green (basaltic) Vatnaöldur horizon (Larsen, 1984; Sigurgeirsson et al., 2013).

TUNU2013 samples included an extended section of ice covering the period 876 to 878 (QUB-1935), and three additional samples that isolated the main microparticle peak (QUB-1972) from ice immediately above and below (Fig. 2M). QUB-1935 contained a mixture of colourless and brown shards, analysis of which confirmed the presence of both components of the Settlement tephra (Fig. 6C). The finer resolution sampling revealed a high concentration (n. >500) of mainly colourless, predominantly cuspate ash in QUB-1972, coincident with peaks in nssS and large microparticles, with a smaller (<5%) proportion of brown ash. Geochemically, the former is consistent with Torfajökull ash, and the latter with Vatnaöldur. Ice immediately below this level (QUB-1973), capturing a smaller microparticle spike, also contained a concentration (n. >80) of greenish-brown shards with a geochemistry matching Vatnaöldur (Fig. 6C). The stratigraphic position of the two components in the ice is therefore inverse to that in Iceland, illustrating different dispersal trajectories of the ash clouds from each system. The TUNU2013 ice core samples demonstrate that the eruption sequence was a protracted event, commencing first in the Bárdarbunga system and extending over a period of about one year.

2.2.13. 649/650 ± 2 Unknown

A prominent particle peak at 650 prompted sampling to investigate the possibility of a useful tephra isochron (Fig. 2N). Two samples (QUB-1940, -1979) were taken across the particle peak. Only one possible brown tephra shard (~25 μm) was recorded in QUB-1940 and less convincing examples in QUB-1979 but no analyses were obtained.

2.2.14. 480 ± 2 Veidivötn-Bárdarbunga

Two samples of ice encompassing a prominent particle peak coeval with a small sulphate signal at 480 were examined (Fig. 2O). QUB-1941 yielded 16 small, pale brown, platy shards, but a greater concentration (n. >200) of greenish-brown, platy to cuspate shards was recovered from QUB-1981. Geochemical analyses from the two samples are consistent with Veidivötn-Bárdarbunga basaltic glass (Fig. 6C). As individual eruptions from this system cannot be distinguished by major element geochemistry, it is not possible to link with certainty the TUNU2013 ash to a specific event. Several Bárdarbunga tephras of imprecise age have been noted in Iceland around this time (Gudmundsdóttir et al., 2016).

2.2.15. 455 ± 2 Shiveluch?

The largest microparticle spike of the first millennium TUNU2013 ice coincides with an extended moderate peak in nssS (Fig. 2P). A substantial concentration (n. >400) of mainly cuspate to vesicular, colourless shards 10–50 μm in maximum length was found in the sample corresponding to the microparticle peak (QUB-1982). The thin glass was prone to burning during analysis, resulting in low analytical totals and elevated Cl, and some shards contained plagioclase and Fe–Ti microlites; only analyses above 93% and not showing element enrichment from minerals are presented here. The major element geochemistry indicates a rhyolitic glass that correlates with Shiveluch, Kamchatka, except for a slightly higher P content. Of the many Shiveluch eruptives around this time, QUB-1982 most closely resembles SH16, dated to around 401 (Ponomareva et al., 2015).

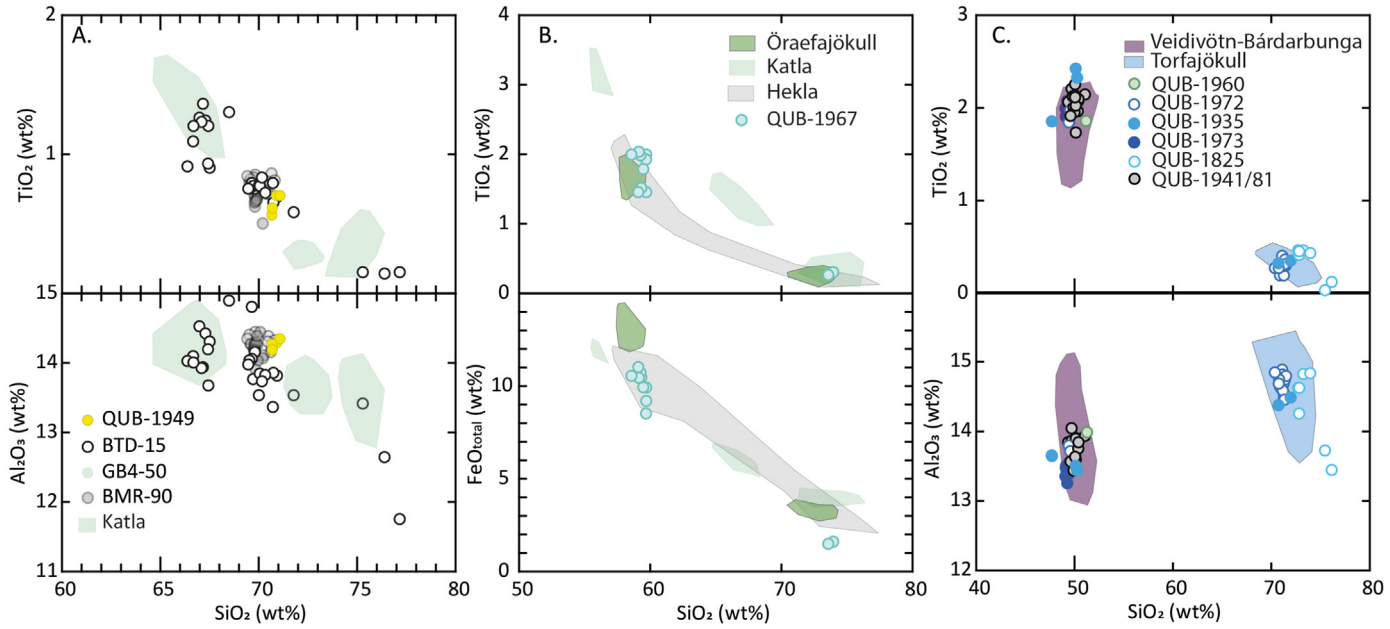

Fig. 6. Major element glass geochemistry of tephras from TUNU2013 and NEEM-2011-S1 plotted against data from Icelandic tephras and cryptotephras in northwest Europe. (A) QUB-1949 plotted against BTD-15 and comparable cryptotephras from northwest Europe (Pilcher et al., 2005; Borgmark and Wastegård, 2008; Fyfe et al., 2016; Watson et al., 2017; Plunkett and Pilcher, 2018) and silicic Katla tephra (Mangerud et al., 1984; Turney et al., 1997; Björck and Wastegård, 1999; Zillén et al., 2002; Wastegård et al., 2000, 2008; Larsen et al., 1999, 2001; Hall and Pilcher, 2002; Wastegård, 2002; Pilcher et al., 2005; Koren et al., 2008; Jennings et al., 2014; Watson et al., 2016; Plunkett and Pilcher, 2018; Moles et al., 2019). Like the European cryptotephra, QUB-1949 lies between two populations of Katla tephra, which are also represented in BTD-15, implying that Katla might be the source of the intermediary populations. (B) QUB-1967 plotted against selected silicic tephras from Iceland (Mangerud et al., 1984; Dugmore et al., 1992; Pilcher et al., 1995, 2005; Dugmore and Newton, 1997; Turney et al., 1997; Wastegård et al., 1998, 2000; Björck and Wastegård, 1999; Larsen et al., 2001; Hall and Pilcher, 2002; Zillén et al., 2002; Koren et al., 2008; Watson et al., 2016; Jónsson et al., 2020). Similarities with the Hekla and Katla fields in particular suggest that QUB-1967 may be of Icelandic origin. (C) QUB-1960, -1935, -1973, -1972, -1941/81 and -1825 plotted against data from Veidivötn-Bárdarbunga and Torfajökull (Boygle, 1994; Dugmore et al., 1995; Pilcher et al., 1996; Hannon et al., 1998; Larsen et al., 1999; Wastegård et al., 2001; van den Bogaard et al., 2002; Wastegård, 2002; Chambers et al., 2004; Gudmundsdóttir et al., 2012; Watson et al., 2016; Wulf et al., 2016); the presence of both components in QUB-1935, -1972 and -1973 is consistent with the Settlement tephra.

2.3. NEEM-2011-S1 previously unpublished tephra

2.3.1. 881 ± 2 Unknown, mixed

A sample of ice corresponding to the sulphate peak associated in the GRIP and GISP2 ice cores with the Settlement tephra (Grönvold et al., 1995; Zielinski et al., 1997b) was examined. The sample contained three colourless, platy shards, two of which were analysed multiple times (QUB-1825). The shards have dissimilar rhyolitic compositions, neither of which clearly match the Torfajökull unit of the Settlement tephra (Fig. 6C). Both show affinities with Kamchatka tephra, although no certain correlation with any specific eruptive was found.

2.3.2. 531 ± 1 Inyo Craters? and Unknown (North Atlantic?)

This interval was examined as part of an investigation into the source of the 536 CE volcanic signal (Sigl et al., 2015). At least nine shards showing variable morphology (cuspate, bubbly-walled, blocky, some microlitic; size range 40–100 μm) were recorded in a sample dating to 531 ± 1, of which three were analysed (QUB-1855). Multiple analyses were obtained on each shard, and demonstrated three heterogenous geochemical compositions, including rhyolitic, trachytic and tephritic. The rhyolitic geochemistry is consistent with that of the Wilson Butte fall deposit associated with the Inyo Craters system, California (Jensen et al., 2021; Fig. 8). Its geochemistry is less evolved than the South Mono tephra from the same system that has recently been identified in northeast America (Jensen et al., 2021). The tephritic shard has a composition similar to the Canaries and the Azores, signifying a possible North Atlantic origin (Fig. 7).

3. Discussion

3.1. Tephra representation in Common Era ice in Greenland

The number of distinct tephras recognised in Common Era Greenland ice cores now stands at 53 (Table 1). As found by Plunkett et al. (2020), microparticle records provide a strong indication that some volcanic ash may be present in the ice. There is no direct correlation between the concentrations of microparticles (<10 μm) and larger (>10 μm) tephra shards, however; large microparticle peaks (in the detectable range up to 10 μm) do not necessarily indicate abundant tephra visible under the microscope (i.e., typically >10 μm). Although they sometimes include ultrafine glass shards, the microparticles themselves may be constituted of other volcanic material such as lithic fragments or phenocrysts; further dedicated research is needed to determine their composition. Alternative sample preparation methods can facilitate the analysis of microparticles, albeit at the expense of analytical accuracy (Iverson et al., 2017). Nevertheless, the microparticle records offer a valuable means of homing in on sections of ice cores that merit tephra investigation, and are particularly useful in terms of visualising the relative timing of particulate and sulphate aerosol deposition in the ice (section 3.2).

The source area of tephras reaching Greenland is extensive (Fig. 1). Of the positively correlated tephras, Iceland is the leading source, yet only eight certain eruptions from this highly volcanic region are represented. Other confirmed sources include Alaska/Aleutians, the Kuriles, China, El Salvador and Mexico, and perhaps California, Kamchatka, Indonesia and Italy, with one or two tephras recognised from each of these regions. The majority of tephras

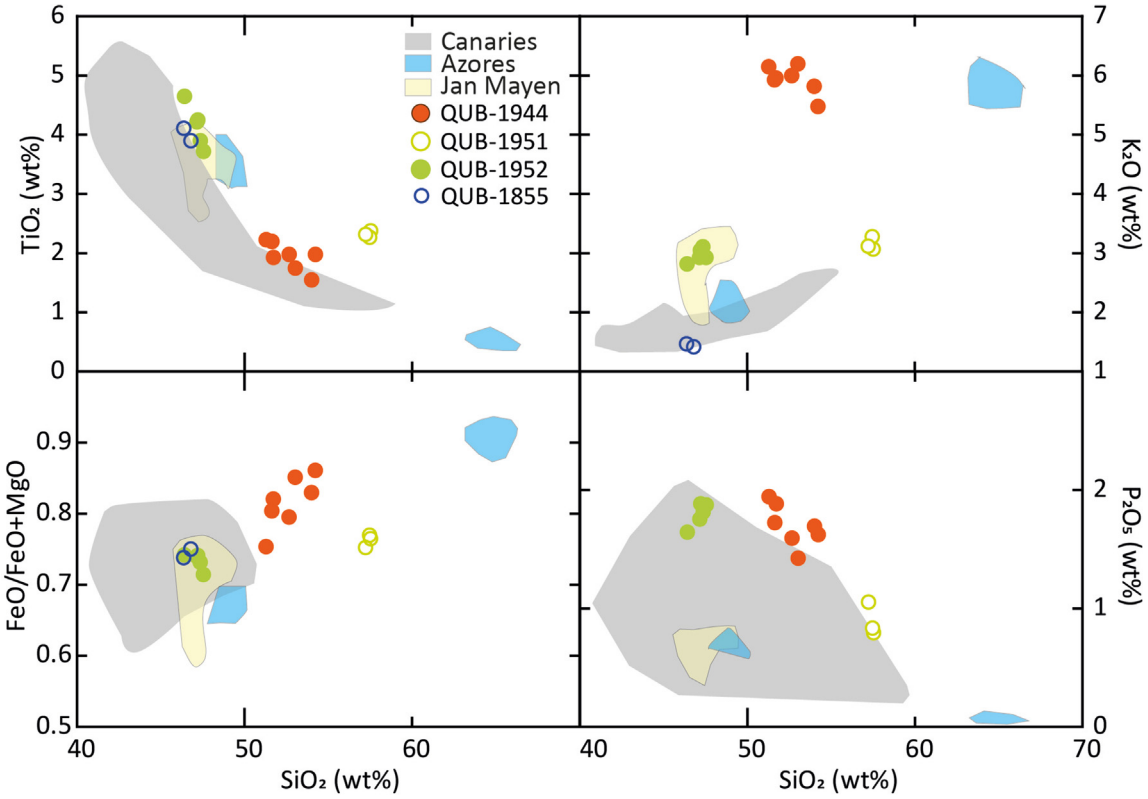

Fig. 7. Major element glass geochemistry of tephras of possible North Atlantic origin. Canaries glass geochemical data are drawn from the EarthChem repository (sources: Martí et al., 2013; Longpré et al., 2014; Del Moro et al., 2015). Jan Mayen data are based on Gjerløw et al. (2015), and Azores data on Tomlinson et al. (2015), Johansson et al. (2017) and Wastegård et al. (2020).

(58%) have not been linked to a source, but several have geochemistries that intimate circum-North Pacific volcanic regions as their provenance. Overall, tephras of known or suspected origins are strongly biased towards mid- or high-latitude Northern Hemisphere volcanoes, but the potential for ash to travel from tropical eruptions is demonstrated by the representation of El Chichón 1982, Ilopango 431 ± 2 and possibly Samalas 1257 (Palais et al., 1992; Zielinski et al., 1997a; Lavigne et al., 2013; Smith et al., 2020).

Difficulties in tying tephras to source based on major element geochemical composition are mainly twofold. Firstly, the major elemental composition of tephras, especially rhyolites, are not always sufficient to distinguish tephras from different volcanic regions, illustrated by similarities in the rhyolitic end-members of Ilopango and Shiveluch (Smith et al., 2020) and by Tamboran and Alaskan tephras (section 2.2.2). In such instances, trace and rare element analysis can resolve the source (Westgate et al., 1994; Pearce et al., 2004b; Plunkett et al., 2017, 2022), but is generally only feasible on larger (>30 μm) shards with sufficient areas of glass free of mineral inclusions. Secondly, successful provenancing of tephras is strongly dependent on the availability of comparative data. Despite the impressive datasets that are now available for Late Holocene tephras from Iceland (e.g., Haflidason et al., 2000; Larsen et al., 2001; Óladóttir et al., 2005, 2008, 2011; Gudmundsdóttir et al., 2016, 2018), Alaska (Cameron et al., 2019) and Kamchatka (e.g., Ponomareva et al., 2015; Krasheninnikov et al., 2020; Portnyagin et al., 2020), not all eruptions, or phases of eruptions, have been captured by proximal analyses. Cryptotephra records from distal locations highlight the occurrence of eruptions not reported from proximal records (Davies et al., 2016; Plunkett and Pilcher, 2018), either because they have escaped attention or have not been preserved locally. Glass data availability from other volcanic regions is relatively limited.

Many examples of rhyolitic tephras displaying high Si (75–77 wt %) and low Fe (0.4–1 wt %) and Ca (0.3–1 wt %) geochemistries are now recognised, not only in Greenland ice but also in European and North American cryptotephra records (Plunkett and Pilcher, 2018; Plunkett et al., 2020; Jensen et al., 2021). Such tephras are known from a wide range of volcanic provenances, including Alaska/the Aleutians, Kamchatka, Japan, Mono-Inyo Craters, Mexico and the Central American Volcanic Area (CAVA), New Zealand, and more rarely from Iceland. The geochemistry also bears a resemblance to Pleistocene-age tephras such as the Bishop Tuff and Wilson Creek, California, USA (Marcaida et al., 2014; Chamberlain et al., 2015), several units from Sambe, Japan (Smith et al., 2013; Albert et al., 2018), as well as various tephras from the Caucasus (Cullen et al., 2014). The recurrence of this type of tephra in low abundance could signify frequent remobilisation of older ash towards Greenland. Detrital ash was recognizable in mid-western American sedimentary records as physically and geochemically altered glass (Jensen et al., 2021). For most of the Greenland tephras for which we have multi-shard or replicate analyses, geochemical consistency and lack of physical evidence for weathering favour the interpretation of the glass as primary airfall, which is frequently supported by elevated sulphur and microparticles (cf. Plunkett et al., 2020). The SB-2 tephra in a northeastern American bog (Jensen et al., 2021) also implies that a primary source lies within the tephra catchment zone of the North Atlantic region. Where shard size permits, trace element analyses may help resolve the question of their provenance.

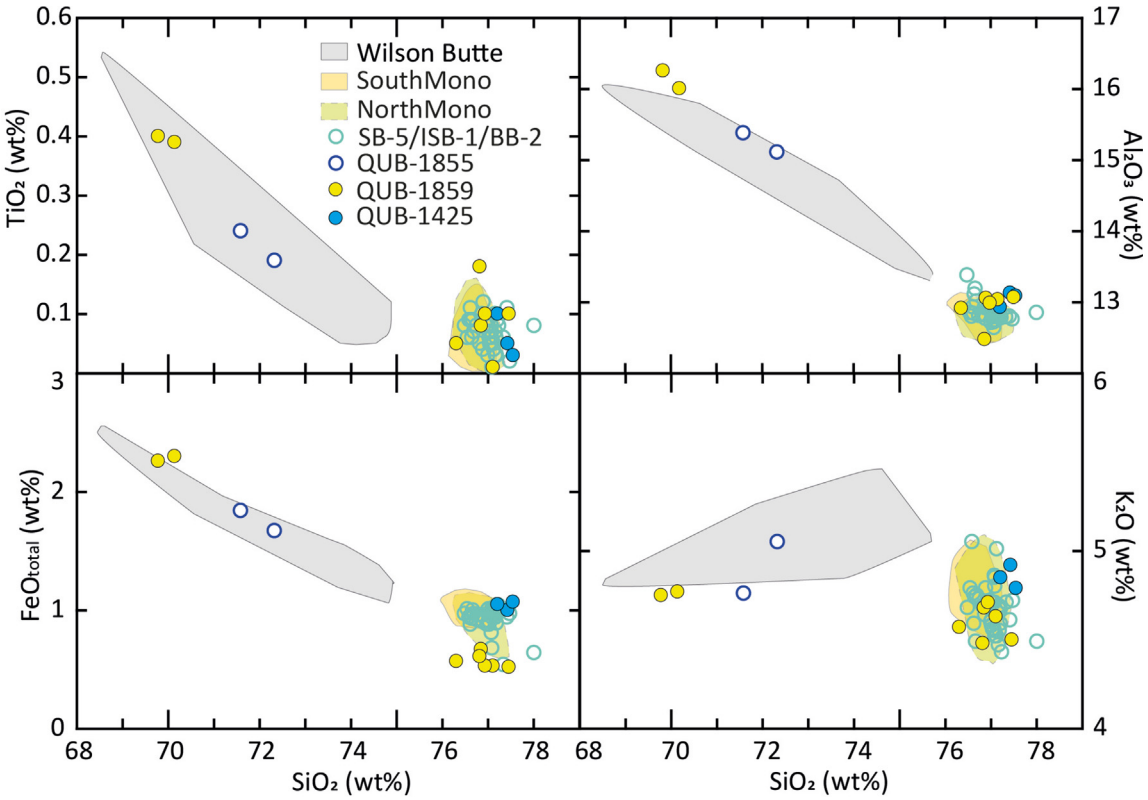

Fig. 8. Major element glass geochemistry for tephras of possible Mono-Inyo Craters origin. North and South Mono and Wilson Butte (Inyo Craters) fields are based on proximal tephra data from Jensen et al. (2021). SB-5/ISB-1/BB-1 cryptotephra from northeast America (Jensen et al., 2021) is of a similar age to QUB-1855 (this paper) and QUB-1859 shards #1, 2, 11 and 12 (Sigl et al., 2015) but QUB-1855 matches the earlier Wilson Butte tephra from Inyo Craters. QUB-1425 (Coulter et al., 2012) is a younger tephra with no correlative in the northeast American cryptotephra record.

3.2. Insights into eruptions represented in Greenland ice

Several large magnitude eruptions of the Common Era have now been confirmed by tephra in Greenland ice cores, including the VEI 7 (or 6; Yang et al., 2021) Millennium Eruption 946 and possibly Samalas 1257, VEI 6 Ilopango 431 ± 2, Churchill 852/3 ± 1 and Novarupta-Katmai 1912 eruptions, and VEI 5 Öraefajökull 1362 (Palais et al., 1991, 1992; Coulter et al., 2012; Sun et al., 2014; Jensen et al., 2014; Smith et al., 2020). Of these, the Millennium Eruption, Churchill and Öraefajökull eruptions are not associated with notable sulphate signals, nor with any remarkable climate impacts (Xu et al., 2013; Mackay et al., 2022). A statistically significant cooling of ~0.3–0.8 °C followed the Churchill eruption, though the effects may have amplified a pre-existing climate anomaly (Mackay et al., 2022). Yet the cooling appears to have been inconsequential from a societal perspective, raising questions about thresholds and conditions for societal perception of and vulnerability to volcanic impacts. These events highlight that not all large magnitude eruptions emit sufficient sulphuric aerosols to trigger an appreciable climate response. Large aerosol emissions from Ilopango, on the other hand, are represented by prominent sulphate spikes in bipolar ice cores that rank amongst the largest volcanic stratospheric sulphate injections in the last 2500 years (Sigl et al., 2015; Toohey and Sigl, 2017; Smith et al., 2020). With fewer historical records for this time interval, short-lived responses to the expected cooling (~0.5 °C) have not been identified. Conversely, the 1257 (1259 in ice cores) Samalas eruption stands out as one of the most impactful events of the Common Era (Sigl et al., 2015; Guillet et al., 2017).

Following the Novarupta-Katmai eruption, the largest magnitude eruption of the 20th century, regional cooling is suggested by Northern Hemisphere tree-ring summer temperature reconstructions and growth anomalies in 1912 and 1913 (LaMarche and Hirschboeck, 1984; Briffa et al., 1998; Büntgen et al., 2020). The cooling appears to be the culmination of a declining trend beginning in 1909 (Büntgen et al., 2020) but, as far as we can determine, has no extra-regional societal repercussions. A comparable stratospheric sulphate injection was estimated for the probably Alaskan 88 ± 2 CE eruption (Plunkett et al., 2022), but in this instance, no climate response is evident in tree-ring summer temperature reconstructions (Büntgen et al., 2020). Although the column altitude of the 88 ± 2 event is not known, it was also likely stratospheric (VEI estimate of ≥4+). A key difference between the events is the longevity of sulphates in the atmosphere: deposition of stratospheric sulphate in Greenland occurred almost a year after the 1912 eruption (Burke et al., 2019) whereas the sulphate deposition in Greenland from the 88 ± 2 eruption dissipated in less than that time (Plunkett et al., 2022). It is likely, therefore, that a large proportion of the sulphate remained tropospheric following the 88 ± 2 eruption or that other factors (e.g., larger aerosol particle sizes) contributed to its more rapid fallout.

The highly variable impacts of the confirmed large magnitude eruptions prompt us to consider the identity of those events with the largest volcanic forcing potential, as determined from sulphate deposition rates in polar ice cores (Sigl et al., 2015, Fig. 9). Although only a small proportion have reported tephras, it is now evident that they include extra-tropical events, including examples of mainly effusive eruptions. Indeed, the two Icelandic fissure eruptions – Eldgjá 939 ± 1 and Laki 1783 – correlate with well-documented examples of climatic and societal repercussions

(Thordarson and Self, 2003; Oppenheimer et al., 2018). Considered VEI 4 events because of their sizeable erupted masses, these eruptions entailed mainly tropospheric emissions, but phases of potentially stratospheric injection were aided by interaction with groundwater that produced explosive phreatomagmatic eruptions (Thordarson et al., 1996, 2001; Moreland et al., 2019). Another noteworthy feature is the frequent co-occurrence of two or more populations of tephra that imply coeval eruptions. In some cases (e.g., 536 Unknowns; Sigl et al., 2015), the sulphate signal structure is consistent with the contribution of aerosols from a single source, but determination of source – needed for refined estimates of stratospheric sulphate loading – is complicated by the multiple contenders suggested by the ash. All in all, tephra has played a significant role in drawing attention to the contribution of extra-tropical eruptions to climate change (Toohey et al., 2016).

While large sulphate emissions are requisite to altering radiative balance, can we learn more about the eruptions that impact climate from the tephra? We have compiled data inferred from the ash and aerosols in Greenland ice cores to investigate characteristics of those eruptions that are robustly associated with climate responses, extending back to the mid-Holocene to increase our sample size (Table 2). The lack of a strong correlation between magnitude and climate response has already been discussed. From our limited dataset, eruption season does not clearly determine the impact. The geochemical composition of the tephra found in Greenland reveals a greater prevalence of mafic to intermediate glass associated with climate impacts, and phreatomagmatic processes are frequently implicated. Magma type determines eruption style, which in turn influences the concentrations of gas species and ash in the plume (Witham et al., 2005; Shinohara, 2008). Interaction with groundwater (phreatomagmatism) may increase the explosivity of an eruption, the additional water content also influencing chemical speciation in the plume. The seemingly muted impact of eruptions producing mid-to high Si rhyolitic tephra may imply that processes relating to magma-gas differentiation in the magma chamber exert an influence on aerosol production and ultimately climate response. Cold anomalies following Churchill and Novarupta-Katmai demonstrate that such eruptions may nonetheless accentuate existing temperature downturns. The Mazama eruption, associated with vesicular rhyolitic tephra, is presently exceptional with respect to its estimated emission of 160 (±50) Tg of sulphur (Sigl et al., 2022). On the other hand, eruptions that produce basaltic tephra can, but do not necessarily, lead to obvious climate perturbations, although the co-occurrence of other dacitic tephras from contemporary eruptions (Zielinski et al., 1994, 1995) complicates the interpretation of these events. Like Eldgjá 939 ± 1 and Laki 1783, the 877 ± 1 co-eruption of Bárdarbunga and Torfajökull, which produced the Settlement tephra, was a protracted event, yet it seems to have had limited climatic and societal repercussions due to lower sulphur yields. Further systematic analysis between the relationship of magma geochemistry, eruption processes, halogen representation in the ice cores, and climate responses may help to discern influential processes affecting climate response.

3.3. Identifying tropical eruptions in polar ice cores

The need for accompanying tephra to confirm the source of a volcanic signal in polar ice cores favours the recognition of extra-tropical eruptions in these records, as several factors work to limit the poleward dispersal of ash from tropical sources. Ash particles that lend themselves to identification using light microscopy and standard microprobe analysis are, by virtue of their greater fall velocities, prone to more rapid settling out of the atmosphere. High water content in a plume increases the aggregation of ash particles, which increases the fall velocities further (Brown et al., 2012). Towards the top of the eruption column, gas and ash clouds frequently separate, the gases usually rising higher than the particles (Prata et al., 2017; Rose et al., 2001). Whether this is due to the contrasting densities of the two components, or the phased eruption of the gases before the particulates, is not clear. Gas and ash components may therefore be transported along separate pathways and at different altitudes. Dispersion modelling suggests that ash is deposited within days to weeks of its eruption (Plunkett et al., 2022), and Niemeier et al. (2009) contend that the residence of even very fine ash (<15 μm) is limited to a matter of weeks. Tropospheric transport direction and fallout is determined chiefly by meteorological conditions at the time of the eruption, limiting the potential for transfer between hemispheres and increasing the rate of sedimentation. Volcanic material injected into the troposphere, including ash, can cross into the stratosphere during transport as a result of convection (Tupper et al., 2009; Carn et al., 2016). Here it has a longer residence; submicron ash particles have been identified in the stratosphere several months after large tropical eruptions (Pueschel et al., 1994; Vernier et al., 2016) and, as noted above, Pinatubo particles <10 μm were sustained for up to three years after the eruption (Cole-Dai et al., 1997). How long larger ash particles can remain suspended is not known. In the tropics, meridional circulation carries the aerosols polewards over the course of one to two years, but expansion to the extra-tropics is

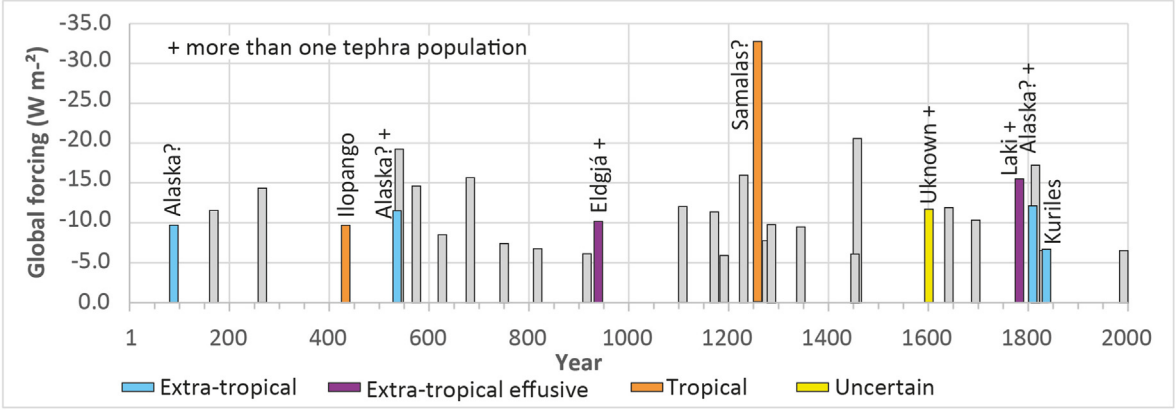

Fig. 9. Largest volcanic eruptions of the Common Era according to sulphate deposition in the polar ice cores (Sigl et al., 2015), highlighting events whose volcanic sources have been confirmed by associated tephras.

Table 2
Attributes of positively identified tephras in Holocene Greenland ice.

	Location	VEI	Season	S (Tg)	Particle relationship to S	Glass composition	Eruption style	>1 eruption?	Tephra reference	Sulphur reference
Eruptions associated with major climate change and societal impacts										
Laki 1783 CE	Extra-tropical	4	Summer to winter	61	Before S peak	Basaltic	Effusive, phreatomagmatic	Yes (dacitic)	Fiacco et al. (1994)	Thordarson and Self (2003)
Unknown (Huaynaputina 1600)	Mixed	(6)	(Spring)	19 ± 4	Uncertain	Dacitic/ Rhyolitic	(Plinian)	Yes	de Silva and Zielinski (1998)	Toohey and Sigl (2017)
Samalas? 1259 CE	Tropical	7	Summer-autumn?	59 ± 11	Synchronous	Trachydacitic-rhyolitic	Phreatomagmatic?	Yes - SH (trachytic, rhyolitic)	Palais et al. (1992)	Toohey and Sigl (2017)
Eldgjá 939 ± 1 CE	Extra-tropical	4	Summer-autumn?	110	Synchronous	Basaltic	Effusive, Strombolian, phreatomagmatic	Yes (dacitic)	Zielinski et al. (1995)	Thordarson et al. (2001)
Unknowns 536 CE	Extra-tropical	≥4+	Autumn-winter?	19 ± 7	Before S peak	Mixed	Unknown	Yes (mixed)	Sigl et al. (2015)	Toohey and Sigl (2017)
Okmok 43 ± 1 BCE	Extra-tropical	6	Winter	48 ± 15	Before S peak	Andesitic	Phreatomagmatic, PDC	No	McConnell et al. (2020)	Pearson et al. (2022)
Aniakchak 1628 or 1627 BCE	Extra-tropical	6	Unknown	52 ± 17	Before S peak	Rhyodacitic and andesitic	Plinian, PDC	No	Pearson et al. (2022)	Pearson et al. (2022)
Mazama ~5677 ± 150 BCE	Extra-tropical	7	Autumn?	162 ± 47	Synchronous	Rhyolitic	Plinian	No	Zdanowicz et al. (1999)	Sigl et al. (2022)
Eruptions associated with small temperature anomalies										
Katmai 1912 CE	Extra-tropical	6	Summer	2.8	Before S peak	Rhyolitic	Plinian	No	Coulter et al. (2012)	volcan-eesm_global_2015_so2-emissions-database_v1
Churchill 852/3 ± 1 CE	Extra-tropical	6	Winter	2.5 ± 0.8	Before S peak	Rhyolitic	Plinian	No	Mackay et al. (2022)	Toohey and Sigl (2017)
Ilopango 431 ± 2 CE	Tropical	6	Unknown	14 ± 2	S > 1 yr later	Rhyolitic and dacitic	Plinian	No	Smith et al. (2020)	Toohey and Sigl (2017)
Eruptions not associated with climate change										
Veidivötn-Bárdarbunga 1477 CE	Extra-tropical	6	Winter	5.1 ± 1.6	Synchronous	Basaltic	Phreatomagmatic	No	Abbott et al. (2021)	Toohey and Sigl (2017)
Öraefajökull 1362 CE	Extra-tropical	5	Summer	<1	Synchronous (low S)	Rhyolitic	Plinian	No	Coulter et al. (2012)	Toohey and Sigl (2017)
ME 946 CE	Extra-tropical	7/6	Winter	1.7 ± 0.6	Synchronous (low S)	Trachytic to rhyodacitic	Plinian	Yes? (rhyolitic)	Sun et al. (2014)	Toohey and Sigl (2017)
Settlement 877 ± 2 CE	Extra-tropical	4	Unknown	1.9 ± 0.7	Synchronous	Rhyolitic and basaltic	Plinian, Phreatomagmatic	No	Grönvold et al. (1995); Zielinski et al. (1997b)	Toohey and Sigl (2017)
Veidivötn-Bárdarbunga 479 ± 2 CE	Extra-tropical	?	Unknown	<1	Synchronous (low S)	Basaltic	Effusive	No	This paper	Toohey and Sigl (2017)
Alaska? 88 ± 2 CE	Extra-tropical	≥4+	Winter	11 ± 4	Synchronous	Andesitic	Plinian/Sub-Plinian?	No	Plunkett et al. (2022)	Toohey and Sigl (2017)
Khangar ~5922 ± 50 BCE	Extra-tropical	6	Unknown	30 ± 8	N/A	Rhyolitic	Plinian?	No	Cook et al. (2018)	Sigl et al. (2022)

restricted by a subtropical transport barrier such that only very high emissions pass into higher latitudes (Marshall et al., 2019). Given the challenges of ash achieving an altitude and residence time sufficient to cross latitudinal zones, it is not surprising that tropical eruptions are poorly represented by tephra in polar ice cores.

Identification of low-latitude eruptions in ice-core records has conventionally been based upon the recognition of concurrent volcanic signals in both polar regions (Langway et al., 1995; Crowley, 2000; Sigl et al., 2013). Contemporaneous extra-tropical eruptions in each hemisphere can, however, give rise to a false impression of a tropical event. It is now also recognised that aerosols from extra-tropical eruptions can pass into the opposite hemisphere and be represented as a bipolar signal (Pearson et al., 2022). Misidentified tropical eruptions will lead to an overestimation of the global radiative forcing potential of an event, as the translation of sulphate deposition rates in polar regions to atmospheric stratospheric loading is dependent on the latitude of the eruption (Toohey et al., 2016; Marshall et al., 2021). Given these issues, we examine whether tropical and extra-tropical eruptions leave discernible signatures in the timing of microparticle and sulphate deposition in the ice cores that might aid the recognition of source distance in the absence of analysable tephra (Fig. 10).

We have small subsets of ash from eruptions in several extra-tropical source regions that provide insights into dispersion rates of volcanic emissions from higher latitudes. Iceland and Jan Mayen represent the closest volcanic sources to Greenland (Fig. 10A). No volcanic sulphates are associated with Öraefajökull tephra in the Dye-3 core from southern Greenland (Coulter et al., 2012), but a substantial microparticle peak in TUNU2013 is directly coeval with a small increase in sulphur concentrations. Veidivötn 1477, Eldgjá, the Settlement tephra and Katla 822 ± 1 coincide directly with sulphate peaks, but Laki tephra was deposited in the early stages of the eruption in the summer of 1783 before sulphate rises (Fiacco et al., 1994). The TUNU2013 record similarly indicates particles arriving in the months before the peak in non-sea-salt sulphur. Veidivötn 1485 ± 1 and 480 ± 2 tephras are not associated with an increase in sulphate. On the whole, particle and chemical fallout from Icelandic eruptions generally seems to be contemporaneous, which likely reflects their rapid deposition following tropospheric transport. Amongst the Alaskan eruptions, Novarupta-Katmai 1912, Churchill 852/3 ± 1, Okmok 43 ± 1 BCE and Aniakchak 1628 or 1627 BCE share similar patterns of deposition: ash is deposited as sulphates start to increase, but peak sulphur deposition is delayed by several months (Fig. 10B). In at least two of these examples (Novarupta-Katmai and Aniakchak), S isotopes reveal that the later sulphates were delivered via stratospheric transport (Burke et al., 2019; Pearson et al., 2022). The Unknown 88 ± 2 tephra of likely Alaskan origin also precedes and overlaps with the start of the nssS rise (Plunkett et al., 2022). Similarly, ash from the Kuriles 1831 ± 1 and possible Shiveluch 455 ± 2 events coincide with muted peaks in nssS (Fig. 10C). Sulphate, halogens and ash from the Millennium Eruption are concurrent in the NEEM-2011-S1 and NGRIP records (Sun et al., 2014).

Of the tropical and possibly tropical tephras (Fig. 10D), Ilopango 431 ± 2 shows a substantial offset between tephra and volcanic sulphur deposition (Smith et al., 2020). Although another eruption might be responsible for sulphate deposition in Greenland 432 ± 2, the ice-core stratospheric sulphur injection estimate (Toohey and Sigl, 2017) is consistent with petrological estimates of sulphur released by the eruption (Smith et al., 2020). The delay implies that tephra was transported towards Greenland rapidly by tropospheric

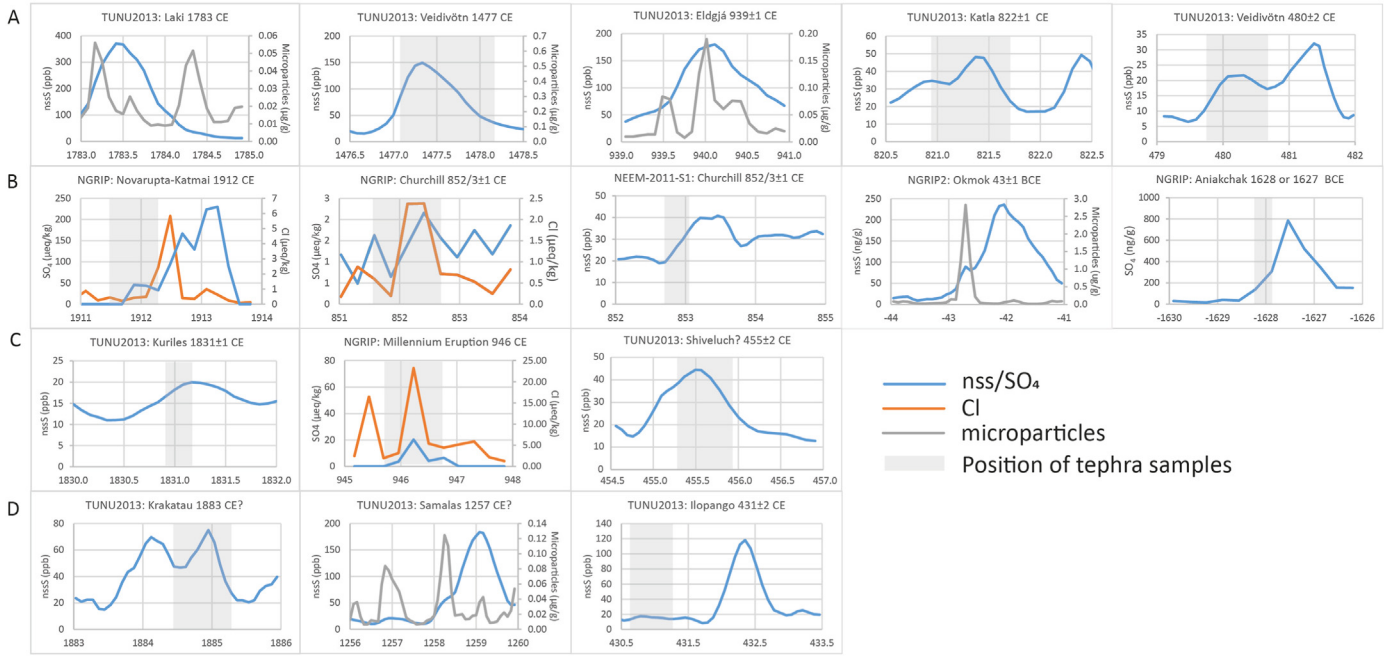

Fig. 10. Temporal relationship between particulate and gas aerosol deposition in Greenland ice cores. X-axes are presented as years (negative values indicate before the Common Era) against NS1-2011 ice core chronology (Sigl et al., 2015), except NGRIP2 which is on the NGRIP2-DRI chronology (McConnell et al., 2018; Sinnl et al., 2022). Chemistry sources are as follows: NGRIP (Vinther et al., 2006; Plummer et al., 2012; Sigl et al., 2015); NGRIP2 (McConnell et al., 2020); NEEM-2011-S1 (Plummer et al., 2012; Sigl et al., 2013, 2015); and TUNU 2013 (Sigl et al., 2015). Positions of geochemically confirmed tephras are shown by shaded bands; due to a lack of available high-resolution data for some GISP2 tephras, TUNU2013 records are shown instead. (A) Icelandic eruptions: Laki 1783 (identified in GISP2 by Fiacco et al., 1994); Veidivötn-Bárdarbunga 1477 CE (Abbott et al., 2021); Eldgjá 939 ± 1 (identified in GISP2 by Zielinski et al., 1995), Katla 822 ± 1 (Plunkett et al., 2020); Veidivötn-Bárdarbunga 480 ± 2 (this paper). (B) Alaskan eruptions: Novarupta-Katmai 1912 (Coulter et al., 2012); Churchill 852/3 ± 1 (Coulter et al., 2012; Jensen et al., 2014); Okmok 43 ± 1 BCE (McConnell et al., 2020); Aniakchak 1628 or 1627 BCE (Pearson et al., 2022). (C) Extra-tropical east Asian eruptions: Shiveluch? 455 ± 2 (this paper); Millennium Eruption 946 (Coulter et al., 2012); Kuriles 1831 (this paper). (D) Tropical and possibly tropical eruptions: Krakatau 1883? (this paper); Samalas 1257? (identified in GISP2 by Palais et al., 1992); Ilopango 431 ± 2 (Smith et al., 2020).

winds, with the sulphates requiring greater time to disperse through the stratosphere. The c. 1259 very fine ash (<6 μm) in GISP2 was found to slightly precede and coincide with sulphur peaks (Palais et al., 1992), signifying a common transport pathway, which sulphur isotopes confirm to be stratospheric (Burke et al., 2019). In TUNU 2013, a peak in microparticles leads the rise in sulphur but has not yet been analysed for tephra. In Antarctica, the ash is confirmed as deriving from the Samalas 1257 eruption (Narcisi et al., 2019), again implying the possibility of a time lapse between a tropical eruption and the deposition of its fallout in the polar regions. We tentatively suggest that the ash and slightly elevated sulphur observed in 1884 and 1885 could derive from Krakatau 1883, but trace element analyses of the shards are required to support this inference (section 2.2.2). On the whole, there is no consistent relationship between the timing of ash and gas aerosol deposition from low-latitude volcanoes in polar regions, but candidate sources for potentially tropical eruptions are very likely to date to at least a year or two before the events are registered as sulphate signals in ice cores. Such an offset has implications for the use of historical volcanic events for dating and estimating error for ice-core chronologies.

3.4. A North Atlantic Common Era tephra framework

Cryptotephra studies in regions either side of the North Atlantic allow examination of intercontinental linkages and ash transport across Greenland (Figs. 1 and 11). The recent synthesis of cryptotephras from northeastern America outlines 14 discrete marker horizons within the Common Era, including ash derived from Mexico, the Cascades and Mono-Inyo Craters, Alaska and the Aleutian Arc, the Kuriles and Kamchatka (Jensen et al., 2021). With a longer history of cryptotephra research, northwest Europe is represented by almost 50 different tephras dating to within the last two millennia, the majority derived from Iceland sources (Plunkett and Pilcher, 2018). Both regions clearly indicate the predominance of tephra emanating from the nearest sources to their west. For comparison, Icelandic records include more than 150 known (and geochemically characterised) tephras in the same timeframe, but many of them from mainly non-explosive, basaltic eruptions from which tephra will have been poorly dispersed. Perched between the two continental regions but at a higher latitude, Greenland is on par with northwest Europe in terms of the number of cryptotephras, but reveals a more varied range of source regions contributing

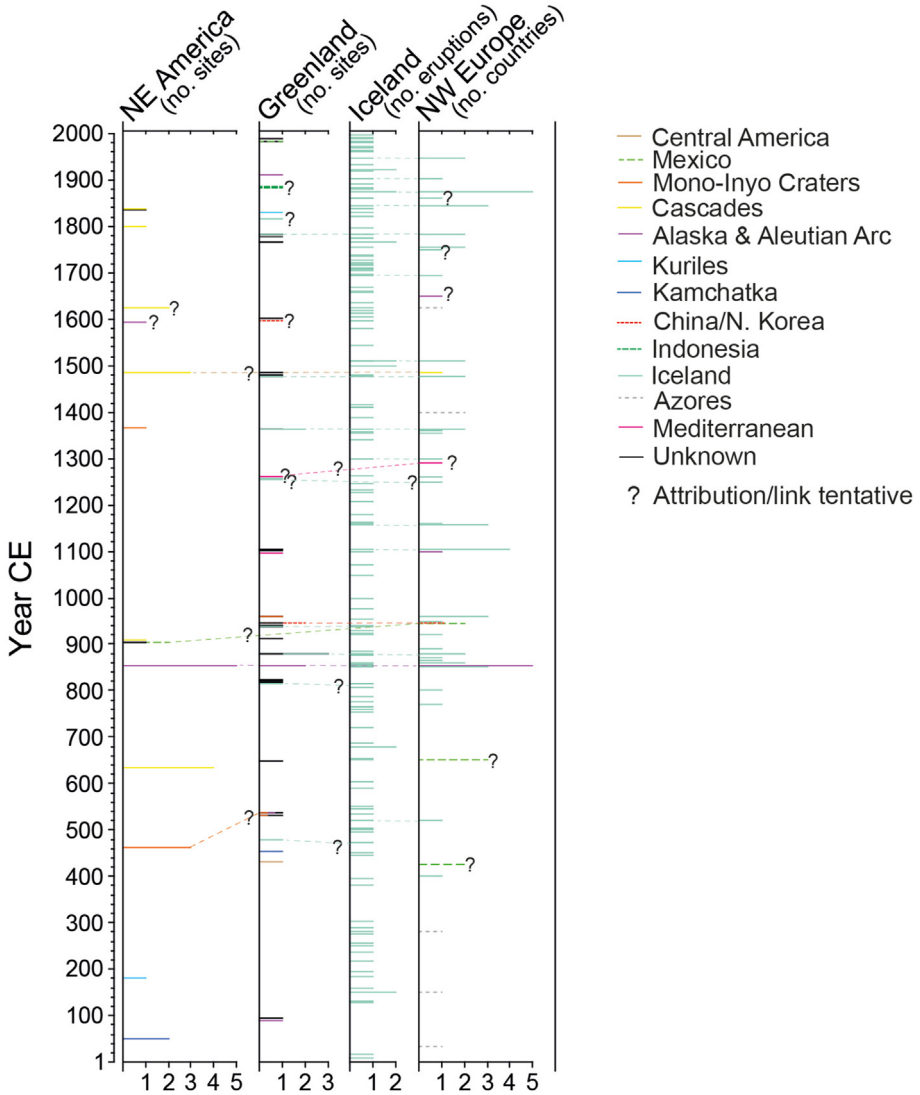

Fig. 11. North Atlantic tephra framework, showing frequency and sources of tephras recognised in northeast America (Jensen et al., 2021), northwest Europe (Plunkett and Pilcher, 2018), Iceland (Óladóttir et al., 2005, 2008, 2014; Gudmundsdóttir et al., 2012, 2016; Schmid et al., 2017) and Greenland (this paper).

cryptotephra to its records despite its large proportion of unprovenanced tephras.

All three regions are so far directly interlinked by only the Churchill 852/3 ± 1 tephra. Northeast America receives a large proportion of ashfall from sources in the Cascades and Mono-Inyo Craters, but few of these seem to extend beyond the continent. Although we were unable to find a linkage with Mount St Helens Set W tephra recorded in northeast America and possibly Ireland (section 2.2.8), other candidate microparticle peaks in this timeframe remain to be examined. Plunkett and Pilcher (2018) suggested a possible correlation between the Jala Pumice tephra from Ceboruco, Mexico, recorded at two northeastern American sites (Mackay et al., 2016; Jensen et al., 2021), and the MOR-T4 tephra in Ireland that includes multiple geochemical populations. The age of the MOR-T4 tephra is now constrained to ~937 ± 10 by its occurrence directly beneath ash from the Millennium Eruption in Ireland (Plunkett, unpublished data; see Cloonoolish Bog age-model in Mackay et al., 2022). The identification of the latter tephra in Ireland provides an additional robust tie-point between northwest Europe and Greenland, and demonstrates potential for the ash to be found in North America. A possible linkage exists between Mono Craters tephra identified in several sites in northeast America and dated to 280–645 CE by Jensen et al. (2021) and some components of the 536 tephra (QUB-1859) in NEEM-2011-S1 (Sigl et al., 2015, Fig. 8). As cryptotephra studies expand in North America, it is likely that further correlations between sites and with sources will increase.

A greater number of linkages between Greenland and northwest Europe are afforded by mainly Icelandic tephras. As yet, no Icelandic tephras appear to have been deposited in northeast America, reflecting the significance of prevailing tropospheric winds to the dispersion of ash. Although Iceland can be ruled out as a source for most of the geochemically characterised but as yet unattributed tephras in the Greenland records, there is clearly potential to establish more ties with Icelandic eruptions and perhaps with northwest Europe. Homogenous basaltic geochemistries from individual volcanic systems (e.g., Grímsvötn, Katla, Krafla, Bárdarbunga-Veidivötn) hinder correlations with specific eruptions, but their representation in Greenland ice will provide an opportunity to explore the nature and frequency of sulphate deposition from small to moderate eruptions and the potential impact of such eruptions on climate.

Changes in the frequency and source regions of the cryptotephras through time may signify shifts in atmospheric circulation patterns. For example, during the first seven centuries CE, tephras recognised in NW Europe mainly derive from non-Icelandic sources, including the Azores. During this time, the frequency of ash clouds passing over Europe appears to have diminished, and ash from Mono-Inyo Craters and El Salvador (Ilopango) reached northern Greenland. With its wider tephra catchment, Greenland is well placed to offer greater insights into changes in ash dispersion patterns.

4. Going forward

4.1. Methodological advances

Research on Greenland tephras in the Common Era, and indeed the Holocene, has tended to be highly selective, targeting very specific time intervals or events. This approach has been necessitated by the vast quantities of ice comprising the current epoch that impede the application of continuous sampling used on other sediment types. Automated microparticle recording in the size range 1–10 μm (McConnell, 2013) now enables a hybrid methodology to be adopted, as these features are strongly aligned with larger ash particles that can enable robust geochemical characterisation. Systematic targeting of ice containing elevated microparticle content promises to deliver a near-continuous record of tephra. Further research is needed to determine 1) the composition of the microparticles, 2) if there is a baseline value of microparticle concentration that increases the chances of recovering larger (i.e., recognizable under the microscope) tephra particles, and 3) the frequency of larger tephra in ice that does not feature elevated microparticle content in the typical detection range of 1–10 μm.

Provenancing of Greenland tephras has frequently proven challenging, limited by a lack of comparable data from potential source regions. The success rate of matching tephras to source will likely increase as more data are published, stimulating links with those working with proximal deposits. Cryptotephra research in continental areas, especially in North America, will very likely increase the number of recognised tephras and allow for greater linkages with Greenland. Efforts are being made within the tephra community to ensure best practice in data collection, analysis and reporting (Wallace et al., 2022), which will greatly facilitate the generation of useful datasets for comparative analysis. Reliable correlations between tephra units are optimised by combining reproducible major and trace element geochemistries and by analysing potential correlatives under the same instrumental conditions to eliminate uncertainties in geochemical matching. Several factors hinder the application of such rigorous standards to the analysis of cryptotephras in polar ice cores, not least the low concentration of shards on which analyses can be performed, but also the small shard sizes that frequently fall below the threshold for successful reliable measurements. Where shard size permits,

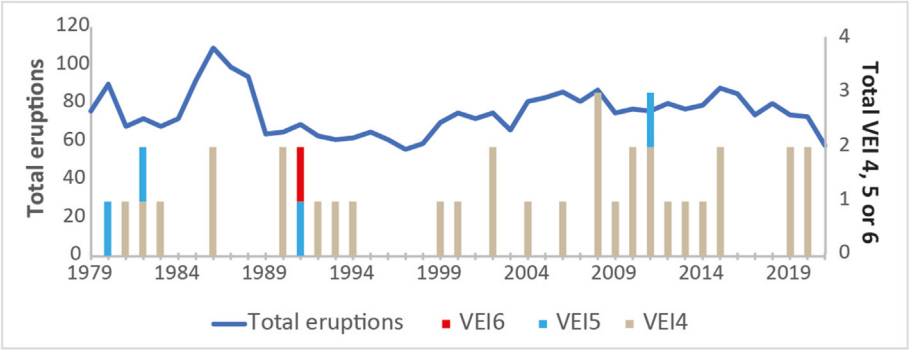

Fig. 12. Number of eruptions since the beginning of satellite recordings in 1978, highlighting the relative infrequency of Volcanic Explosivity Index (VEI) 4, 5 and 6 eruptions (based on Siebert et al., 2010; Global Volcanism Program Database).

reproducibility of major element geochemistry can be tested by obtaining multiple analyses from individual shards. Such small datasets nevertheless present an obstacle to identifying the potential source of the tephra, a prerequisite to obtaining reference material from the source for co-analysis. These limitations aside, a programme of trace element analysis for unprovenanced tephras will help resolve questions of origin and thereby enhance the inferences that can be drawn from the volcanic histories recorded in polar ice cores.

4.2. Learning from tephra

The application of tephra analysis of polar ice cores offers considerable potential to go beyond merely provenancing volcanic signals in the ice. Microparticle records suggest that there are many more volcanic events recorded in Greenland ice than those represented only by clear sulphate peaks, and that multiple eruptions can lie behind some of the more prominent events. Ash dispersion modelling demonstrates that VEI 4 eruptions are sufficient to disperse fine ash to Greenland from a number of Northern Hemisphere sources (Plunkett et al., 2022), and potentially VEI 2 or 3 Icelandic eruptions injected to at least 4 km height (Stevenson et al., 2013). Such eruptions occur on a greater frequency – sub-annual to decadal – than large magnitude eruptions. Currently, climate models incorporate a non-zero minimum stratospheric aerosol depth for periods of "no volcanic eruptions" based on values determined for an evidently quiescent period of volcanism between 1999 and 2005 (Thomason et al., 2018), yet this interval was not quiescent in terms of its total number of eruptions (Fig. 12). The sulphate contributions of effusive eruptions (VEI 0–2) have generally not been quantified from satellite data as they are believed to have minimal impact on stratosphere dynamics (Toohey et al., 2013; Carn et al., 2016; Arias et al., 2021). Numerous empirical and modelling studies have, however, reported the effects of tropospheric sulphates on the radiative properties of meteorological clouds (e.g., Pinto et al., 1989; Schmidt et al., 2012; Malavelle et al., 2017; Chen et al., 2022) and the impacts of small eruptions on climate have only recently begun to be considered. Indeed, the 2014–2015 Holuhraun eruption (VEI 0) in Iceland has been linked to a reduction in cloud droplets, resulting in a modest reduction in global mean radiative forcing (Malavelle et al., 2017). Schmidt et al. (2018) modelled the effects of all small to moderate (injection height >10 km, VEI 3, 4 and 5) eruptions over the period 2000–2015 to determine climate responses in the absence of large magnitude eruptions. They found a small but significant cooling effect resulting from aerosol-cloud interactions in the tropopause that had been overlooked in previous models. It is likely that current baseline estimates for pre-industrial period volcanic forcing (Jungclaus et al., 2017; Arias et al., 2021) underestimate the frequency and contributions of small-to-moderate eruptions. Continuous tephra sampling, guided by microparticle records, of the ice cores could begin to address this issue through the detection of smaller eruptions and their potential contribution to the sulphate content recorded in the ice cores.

Tephra research has been pivotal in the recognition of extra-tropical eruption impacts on climate (Toohey et al., 2019). With many remaining uncertainties regarding the plume-atmosphere-climate relationships, a more holistic analysis of tephra may elucidate critical features of an eruption that make it more likely to have a climate impact. Because volatile concentrations released in an eruption are determined by the geological setting of the volcano, general inferences can be drawn about an event if its source is known, including its likely volatile content and its eruption history. More detailed information about the state of the magma (bubble- or microlite-rich, reflecting the rate of depressurisation) at the moment of eruption can be inferred from the morphology of the tephra shards. The size, shape, vesicularity and geochemistry of ash particles can also influence the efficiency of adsorption of gas compounds, especially those of sulphur, chlorine and fluorine (Witham et al., 2005; Brown et al., 2012). Adsorption reduces volatile concentrations in the plume by significant proportions (De Hoog et al., 2001; Brown et al., 2012; Gutiérrez et al., 2016), but sequestered sulphur dioxide may later be oxidised in the cloud, prolonging the formation of aerosol (De Hoog et al., 2001). As yet, there has been no systematic attempt to record shard morphology in ice-core tephras or to investigate its significance in relation to eruption style or processes, or in moderating the dispersion or impact of volatiles. Further research in this area is needed to maximise our understanding of volcano-climate interactions.

To determine the impact of past eruptions on climate, improved constraints on stratospheric sulphate loading are necessary (Marshall et al., 2019). Better knowledge of the relationship between various volcanic fallout fractions in the ice cores, coupled with sulphur isotope analysis, may provide a mechanism for determining the relative contributions of stratospheric input from the stratigraphical position of ash and volatiles, as well as the role of ash in sequestering chemical compounds from the plume (section 3.4). Furthermore, a more complete record of volcanism will facilitate evaluation of the constancy of atmospheric circulation patterns through the Common Era via the frequency of fallout from different sources regions. The development of ash dispersion modelling to interrogate the meteorological conditions favouring long-distance tephra transport between regions will aid this enquiry. In the Common Era, peak warming in the Northern Hemisphere – the Roman Warm Period, the Medieval Climate Anomaly – coincides with a lower record of sulphate deposition in the Greenland ice cores or with an absence of frequent large tropical eruptions, while cold periods – Late Antique Little Ice Age and the Little Ice Age – feature multi-decadal cooling following large eruptions (Miller et al., 2012; Büntgen et al., 2016; Otto-Bliesner et al., 2016; Kobashi et al., 2017; Brönnimann et al., 2019). Volcanic forcing is considered to be a driver, rather than a response, to such changes, but associated changes in Arctic and North Atlantic Oscillation patterns may influence the nature of the volcanic record in Greenland.

We conclude by considering the challenges of determining when a *statistically* significant climate response to volcanic forcing becomes a *societally* significant issue. With advances in palaeoclimate reconstructions and climate modelling, it is now possible to visualise the spatial variability in climate responses and to identify which areas experienced the greatest anomalies (e.g., McConnell et al., 2020; Timmreck et al., 2021; Mackay et al., 2022; Stoffel et al., 2022). The extent to which such events impact societies, or are even perceptible to societies, is less straightforward, however. In terms of assessing societal vulnerability to volcanic forcing, we need a better handle on threshold values that render populations in different regions susceptible to short-term climate variability: how much warmer, colder, wetter or drier does it need to get before the conditions substantially affect the day-to-day life of populations or the workings of a society? It is equally important to consider the societal conditions – for example, social structure, governance, economic strategies – that leave populations well positioned to adapt, or alternatively vulnerable, to environmental perturbations if we are to prepare for responses to major volcanic forcing in the future.

5. Conclusions

The identification of tephras in ice cores greatly aids the refinement of eruption source parameters for modelling the

impacts of past eruptions represented by sulphate deposition in Greenland ice. A growing number of Common Era tephras from Greenland ice cores are revealing a wide catchment area for tephras reaching the North Atlantic. Extra-tropical Northern Hemisphere tephras predominate amongst whose sources could be identified, but a large proportion remain unprovenanced, reflecting in part the extensive source region but also the relative youth of detailed cryptotephra research in Late Holocene Greenland ice. Although fewer in number, tephras from tropical eruptions can on occasion be deposited in the high latitudes. We validate the usefulness of microparticle records for identifying the likely position of tephras, and for defining the timing of particle deposition relative to other volcanic emissions in the ice. These records will greatly expedite the isolation of tephras, providing a more complete recognition of the frequency of past volcanism, including the occurrence of extra-tropical small-to-moderate eruptions.

From the current dataset of Mid-to Late Holocene tephras, we consider insights into some large magnitude eruptions. We find that magnitude alone is a poor indicator of volcanic impact on climate, and that eruptions producing very viscous, silicic tephra often tend not to result in a noteworthy climate response. Instead, it is intermediate to mafic tephras that are associated with climate and societal impacts. Phreatomagmatic eruptions and the occurrence of multiple eruptions are also recurrent features of the more impactful events. We encourage greater inter-disciplinary collaborations between ice core scientists, tephrochronologists, volcanologists and the ash hazard communities to maximise the inferences that can be drawn from tephra found in ice cores and other sedimentary deposits. Through its geochemistry and morphology, tephra entraps information about the magma source and its evolution and eruption style, and a holistic study of the ash could foster a better understanding of volatile release, plume dynamics and aerosol interactions. Closer scrutiny of the temporal relationship of volcanic emissions in the ice cores provides an opportunity to investigate transport pathways and the potential role of ash in sequestering and transporting gas compounds. There is scope to develop ash dispersion models to interrogate the significance of meteorological conditions in contributing to volcanic signals in the ice cores. All-in-all, the insights afforded by tephra in ice cores could be instrumental in the development of volcano-atmosphere models for reconstructing and predicting volcanic impacts on climate and society.

Author statement

Gill Plunkett: Conceptualization; Methodology; Formal analysis; Investigation; Data curation; Writing – original draft; Writing – review & editing. Michael Sigl: Conceptualization; Formal analysis; Investigation; Data curation; Writing – original draft; Writing – review & editing. Joseph R. McConnell: Resources; Formal analysis; Data curation; Writing – review & editing. Jonathan R. Pilcher: Formal analysis; Writing – review & editing. Nathan J. Chellman: Methodology; Writing – review & editing.

Declaration of competing interest

The authors declare that they have no known competing financial interests or personal relationships that could have appeared to influence the work reported in this paper.

Data availability

Data will be made available on request.

Acknowledgements

This research benefitted from the participation of some of the authors in the Volcanic Impacts on Climate and Society (VICS) working group of the Past Global Changes (PAGES) project. Michael Sigl received funding from the European Research Council under the European Union's Horizon 2020 research and innovation programme (grant agreement no. 820047) and from the Geoscience Department and the NFR TOPPFORK project "VIKINGS" (grant no. 275191) at the University of Oslo. The collection and analysis of the TUNU2013 and NEEM-2011-S1 core were supported by US National Science Foundation grants (nos. 1204176, 909541) to Joseph R. McConnell, with additional support provided (grant no. 1925417) to Joseph R. McConnell and Nathan J. Chellman for the volcanic interpretation. We thank M. Twickler and the National Science Foundation-ICF for providing access to archived TUNU2013 samples, and O. Maselli, R. Rhodes and Beth Bergeron for drilling the Tunu13 cores. Our field team received valuable assistance from CHM2HILL and Ken Borek Air. We thank S.-B. Hansen, T. Popp, D. Mandeno, M. Leonhardt, and A. Moy for drilling the NEEM-2011-S1 core. NEEM is directed and organized by the Center of Ice and Climate at the Niels Bohr Institute and US National Science Foundation, Office of Polar Programs. It is supported by funding agencies and institutions in Belgium (Fund for Scientific Research—French-speaking and Community and Research Foundation—Flanders), Canada (Natural Resources Canada/Geological Survey of Canada), China (Chinese Academy of Sciences), Denmark (Agency for Science and Higher Education), France (Paul-Emile Victor French Polar Institute, French National Centre for Scientific Research/National Institute for Earth Sciences and Astronomy, French Alternative Energies and Atomic Energy Commission and the French National Research Agency), Germany (Alfred Wegener Institute), Iceland (RannIs), Japan (National Institute of Polar Research), Korea (Korean Polar Research Institute), The Netherlands (Dutch Research Council/Earth and Life Sciences Division), Sweden (Swedish Research Council), Switzerland (Swiss National Science Foundation), United Kingdom (Natural Environment Research Council) and the USA (US National Science Foundation, Office of Polar Programs). We are grateful to Alina Schilling, Chris Hayward and Victoria Smith for support with tephra geochemical analysis, Vera Ponomareva for comments on some of the data, and Helen Essell for preparing Fig. 1.

Appendix A. Supplementary data

Supplementary data to this article can be found online at https://doi.org/10.1016/j.quascirev.2022.107936.

References

Abbott, P.M., Davies, S.M., 2012. Volcanism and the Greenland ice-cores: the tephra record. Earth Sci. Rev. 115, 173–191.

Abbott, P.M., Davies, S.M., Steffensen, J.P., Pearce, N.J.G., Bigler, M., Johnsen, S.J., Seierstad, I.K., Svensson, A., Wastegård, S., 2012. A detailed framework of Marine Isotope Stages 4 and 5 volcanic events recorded in two Greenland ice-cores. Quat. Sci. Rev. 36, 59–77.

Abbott, P.M., Plunkett, G., Corona, C., Chellman, N.J., McConnell, J.R., Pilcher, J.R., Stoffel, M., Sigl, M., 2021. Cryptotephra from the Icelandic Veiðivötn 1477 CE eruption in a Greenland ice core: confirming the dating of volcanic events in the 1450s CE and assessing the eruption's climatic impact. Climate Past 17, 565–585.

Albert, P.G., Smith, V.C., Suzuki, T., Tomlinson, E.L., Nakagawa, T., McLean, D., Yamada, M., Staff, R.A., Schlolaut, G., Takemura, K., Nagahashi, Y., 2018. Constraints on the frequency and dispersal of explosive eruptions at Sambe and Daisen volcanoes (South-West Japan Arc) from the distal Lake Suigetsu record (SG06 core). Earth Sci. Rev. 185, 1004–1028.

Arias, P.A., Bellouin, N., Coppola, E., Jones, R.G., Krinner, G., Marotzke, J., Naik, V., Palmer, M.D., Plattner, G.-K., Rogelj, J., Rojas, M., Sillmann, J., Storelvmo, T., Thorne, P.W., Trewin, B., Achuta Rao, K., Adhikary, B., Allan, R.P., Armour, K., Bala, G., Barimalala, R., Berger, S., Canadell, J.G., Cassou, C., Cherchi, A., Collins, W., Collins, W.D., Connors, S.L., Corti, S., Cruz, F., Dentener, F.J.,

Dereczynski, C., Di Luca, A., Diongue Niang, A., Doblas-Reyes, F.J., Dosio, A., Douville, H., Engelbrecht, F., Eyring, V., Fischer, E., Forster, P., Fox-Kemper, B., Fuglestvedt, J.S., Fyfe, J.C., Gillett, N.P., Goldfarb, L., Gorodetskaya, I., Gutierrez, J.M., Hamdi, R., Hawkins, E., Hewitt, H.T., Hope, P., Islam, A.S., Jones, C., Kaufman, D.S., Kopp, R.E., Kosaka, Y., Kossin, J., Krakovska, S., Lee, J.-Y., Li, J., Mauritsen, T., Maycock, T.K., Meinshausen, M., Min, S.-K., Monteiro, P.M.S., Ngo-Duc, T., Otto, F., Pinto, I., Pirani, A., Raghavan, K., Ranasinghe, R., Ruane, A.C., Ruiz, L., Sallée, J.-B., Samset, B.H., Sathyendranath, S., Seneviratne, S.I., Sörensson, A.A., Szopa, S., Takayabu, I., Tréguier, A.-M., van den Hurk, B., Vautard, R., von Schuckmann, K., Zaehle, S., Zhang, X., Zickfeld, K., 2021. Technical summary. In: Masson-Delmotte, V., Zhai, P., Pirani, A., Connors, S.L., Péan, C., Berger, S., Caud, N., Chen, Y., Goldfarb, L., Gomis, M.I., Huang, M., Leitzell, K., Lonnoy, E., Matthews, J.B.R., Maycock, T.K., Waterfield Yelekçi, T.O., Yu, R., Zhou, B. (Eds.), Climate Change 2021: the Physical Science Basis. Contribution of Working Group I to the Sixth Assessment Report of the Intergovernmental Panel on Climate Change. Cambridge University Press, Cambridge, pp. 33–144.

Aubry, T.J., Toohey, M., Marshall, L., Schmidt, A., Jellinek, A.M., 2020. A new volcanic stratospheric sulfate aerosol forcing emulator (EVA_H): comparison with interactive stratospheric aerosol models. J. Geophys. Res.: Atmos. 125, e2019JD031303.

Barbante, C., Kehrwald, N.M., Marianelli, P., Vinther, B.M., Steffensen, J.P., Cozzi, G., Hammer, C.U., Clausen, H.B., 2013. Greenland ice core evidence of the 79 AD Vesuvius eruption. Climate Past 9, 1221–1232.

Baroni, M., Thiemens, M.H., Delmas, R.J., Savarino, J., 2007. Mass-independent sulfur isotopic compositions in stratospheric volcanic eruptions. Science 315, 84–87.

Baroni, M., Savarino, J., Cole-Dai, J.H., Rai, V.K., Thiemens, M.H., 2008. Anomalous sulfur isotope compositions of volcanic sulfate over the last millennium in Antarctic ice cores. J. Geophys. Res.: Atmos. 113, D20112.

Björck, J., Wastegård, S., 1999. Climate oscillations and tephrochronology in eastern middle Sweden during the last glacial–interglacial transition. J. Quat. Sci. 14, 399–410.

Blake, S., 1984. Magma mixing and hybridization processes at the alkalic, silicic, Torfajökull central volcano triggered by tholeiitic Veidivötn fissuring, south Iceland. J. Volcanol. Geoth. Res. 22, 1–31.

Borgmark, A., Wastegård, S., 2008. Regional and local patterns of peat humification in three raised peat bogs in Värmland, south-central Sweden. GFF 130, 161–176.

Bourne, A.J., Cook, E., Abbott, P.M., Seierstad, I.K., Steffensen, J.P., Svensson, A., Fischer, H., Schüpbach, S., Davies, S.M., 2015. A tephra lattice for Greenland and a reconstruction of volcanic events spanning 25–45 ka b2k. Quat. Sci. Rev. 118, 122–141.

Boygle, J.E., 1994. Tephra in Lake Sediments: an Unambiguous Geochronological Marker? PhD Thesis. University of Edinburgh.

Brenna, H., Kutterolf, S., Mills, M.J., Krüger, K., 2020. The potential impacts of a sulfur- and halogen-rich supereruption such as Los Chocoyos on the atmosphere and climate. Atmos. Chem. Phys. 20, 6521–6539.

Briffa, K.R., Jones, P.D., Schweingruber, F.H., Osborn, T.J., 1998. Influence of volcanic eruptions on Northern Hemisphere summer temperature over the past 600 years. Nature 393, 450–455.

Brönnimann, S., Brönnimann, S., Franke, J., Nussbaumer, S.U., Zumbühl, H.J., Steiner, D., Trachsel, M., Hegerl, G.C., Schurer, A., Worni, M., Malik, A., Flückiger, J., 2019. Last phase of the Little Ice Age forced by volcanic eruptions. Nat. Geosci. 12, 650–656.

Brown, R.J., Bonadonna, C., Durant, A.J., 2012. A review of volcanic ash aggregation. Phys. Chem. Earth 45, 65–78.

Büntgen, U., Myglan, V.S., Ljungqvist, F.C., McCormick, M., Di Cosmo, N., Sigl, M., Jungclaus, J., Wagner, S., Krusic, P.J., Esper, J., Kaplan, J.O., de Vaan, M.A.C., Luterbacher, J., Wacker, L., Tegel, W., Kirdyanov, A.V., 2016. Cooling and societal change during the Late Antique Little Ice Age from 536 to around 660 AD. Nat. Geosci. 9, 231–236.

Büntgen, U., Eggertsson, Ó., Wacker, L., Sigl, M., Ljungqvist, F.C., Di Cosmo, N., Plunkett, G., Krusic, P.J., Newfield, T.P., Esper, J., Lane, C., Reinig, F., Oppenheimer, C., 2017. Multi-proxy dating of Iceland's major pre-settlement Katla eruption to 822–823 CE. Geology 45, 783–786.

Büntgen, U., Arseneault, D., Boucher, É., Churakova, O.V., Gennaretti, F., Crivellaro, A., Hughes, M.K., Kirdyanov, A.V., Klippel, L., Krusic, P.J., Linderholm, H.W., Ljungqvist, F.C., Ludescher, J., McCormick, M., Myglan, V.S., Nicolussi, K., Piermattei, A., Oppenheimer, C., Reinig, F., Sigl, M., Vaganov, E.A., Esper, J., 2020. Prominent role of volcanism in Common Era climate variability and human history. Dendrochronologia 64, 125757.

Burke, A., Moore, K.A., Sigl, M., Nita, D.C., McConnell, J.R., Adkins, J.F., 2019. Stratospheric eruptions from tropical and extra-tropical volcanoes constrained using high-resolution sulfur isotopes in ice cores. Earth Planet Sci. Lett. 521, 113–119.

Cameron, C.E., Mulliken, K.M., Crass, S.W., Schaefer, J.R., Wallace, K.L., 2019. Alaska Volcano Observatory geochemical database, version 2. In: Alaska Division of Geological & Geophysical Surveys Digital Data Series, 8, p. 22.

Carn, S.A., Clarisse, L., Prata, A.J., 2016. Multi-decadal satellite measurements of global volcanic degassing. J. Volcanol. Geoth. Res. 311, 99–134.

Chamberlain, K.J., Wilson, C.J., Wallace, P.J., Millet, M.A., 2015. Micro-analytical perspectives on the Bishop Tuff and its magma chamber. J. Petrol. 56, 605–640.

Chambers, F.M., Daniell, J.R.G., Hunt, J.B., Molloy, K., O'Connell, M., 2004. Tephrostratigraphy of an Loch Mór, Inis Oírr, western Ireland: implications for Holocene tephrochronology in the northeastern Atlantic region. Holocene 14, 703–720.

Chen, Y., Haywood, J., Wang, Y., Malavelle, F., Jordan, G., Partridge, D., Fieldsend, J., De Leeuw, J., Schmidt, A., Cho, N., Oreopoulos, L., Platnick, S., Grosvenor, D., Field, P., Lohmann, U., 2022. Machine learning reveals climate forcing from aerosols is dominated by increased cloud cover. Nat. Geosci. 15, 609–614.

Clyne, M., Lamarque, J.F., Mills, M.J., Khodri, M., Ball, W., Bekki, S., Dhomse, S.S., Lebas, N., Mann, G., Marshall, L., Niemeier, U., Poulain, V., Robock, A., Rozanov, E., Schmidt, A., Stenke, A., Sukhodolov, T., Timmreck, C., Toohey, M., Tummon, F., Zanchettin, D., Zhu, Y., Toon, O.B., 2021. Model physics and chemistry causing intermodel disagreement within the VolMIP-Tambora Interactive Stratospheric Aerosol ensemble. Atmos. Chem. Phys. 21, 3317–3343.

Cole-Dai, J., Mosley-Thompson, E., Thompson, L.G., 1997. Quantifying the Pinatubo volcanic signal in south polar snow. Geophys. Res. Lett. 24, 2679–2682.

Cole-Dai, J., Ferris, D., Lanciki, A., Savarino, J., Baroni, M., Thiemens, M.H., 2009. Cold decade (AD 1810–1819) caused by Tambora (1815) and another (1809) stratospheric volcanic eruption. Geophys. Res. Lett. 36, L22703.

Cook, E., Portnyagin, M., Ponomareva, V., Bazanova, L., Svensson, A., Garbe-Schönberg, D., 2018. First identification of cryptotephra from the Kamchatka Peninsula in a Greenland ice core: implications of a widespread marker deposit that links Greenland to the Pacific northwest. Quat. Sci. Rev. 181, 200–206.

Cook, E., Abbott, P.M., Pearce, N.J., Mojtabavi, S., Svensson, A., Bourne, A.J., Rasmussen, S.O., Seierstad, I.K., Vinther, B.M., Harrison, J., Street, E., 2022. Volcanism and the Greenland ice cores: a new tephrochronological framework for the last glacial-interglacial transition (LGIT) based on cryptotephra deposits in three ice cores. Quat. Sci. Rev. 292, 107596.

Coulter, S.E., Pilcher, J.R., Plunkett, G., Baillie, M.G.L., Hall, V.A., Steffensen, J.P., Vinther, B.M., Clausen, H.B., Johnsen, S.J., 2012. Holocene tephras highlight complexity of volcanic signals in Greenland ice cores. J. Geophys. Res.: Atmos. 117, D21303.

Crowley, T.J., 2000. Causes of climate change over the past 1000 years. Science 289, 270–277.

Cullen, V.L., Smith, V.C., Arz, H.W., 2014. The detailed tephrostratigraphy of a core from the south-east Black Sea spanning the last~ 60 ka. J. Quat. Sci. 29, 675–690.

Davies, S.M., Wastegård, S., Abbott, P.M., Barbante, C., Bigler, M., Johnsen, S.J., Rasmussen, T.L., Steffensen, J.P., Svensson, A., 2010. Tracing volcanic events in the NGRIP ice-core and synchronising North Atlantic marine records during the last glacial period. Earth Planet Sci. Lett. 294, 69–79.

Davies, S.M., Abbott, P.M., Meara, R.H., Pearce, N.J., Austin, W.E., Chapman, M.R., Svensson, A., Bigler, M., Rasmussen, T.L., Rasmussen, S.O., Farmer, E.J., 2014. A North Atlantic tephrostratigraphical framework for 130–60 ka b2k: new tephra discoveries, marine-based correlations, and future challenges. Quat. Sci. Rev. 106, 101–121.

Davies, L.J., Jensen, B.J., Froese, D.G., Wallace, K.L., 2016. Late Pleistocene and Holocene tephrostratigraphy of interior Alaska and Yukon: key beds and chronologies over the past 30,000 years. Quat. Sci. Rev. 146, 28–53.

De Angelis, M., Fehrenbach, L., Jehanno, C., Maurette, M., 1985. Micrometre-sized volcanic glasses in polar ices and snows. Nature 317, 52–54.

De Hoog, J.C.M., Koetsier, G.W., Bronto, S., Sriwana, T., Van Bergen, M.J., 2001. Sulfur and chlorine degassing from primitive arc magmas: temporal changes during the 1982–1983 eruptions of Galunggung (West Java, Indonesia). J. Volcanol. Geoth. Res. 108, 55–83.

Del Moro, S., Di Roberto, A., Meletlidis, S., Pompilio, M., Bertagnini, A., Agostini, S., Ridolfi, F., Renzulli, A., 2015. Xenopumice erupted on 15 October 2011 offshore of El Hierro (Canary Islands): a subvolcanic snapshot of magmatic, hydrothermal and pyrometamorphic processes. Bull. Volcanol. 77, 1–19.

De Silva, S.L., Zielinski, G.A., 1998. Global influence of the AD 1600 eruption of Huaynaputina, Peru. Nature 393, 455–458.

Dörfler, W., Feeser, I., van den Bogaard, C., Dreibrodt, S., Erlenkeuser, H., Kleinmann, A., Merkt, J., Wiethold, J., 2012. A high-quality annually laminated sequence from Lake Belau, Northern Germany: revised chronology and its implications for palynological and tephrochronological studies. Holocene 22, 1413–1426.

Dugmore, A., Newton, A., 1997. Holocene tephra layers in the Faroe Islands. Fróðskaparrit 45, 141–154.

Dugmore, A.J., Newton, A.J., Sugden, D.E., Larsen, G., 1992. Geochemical stability of fine-grained silicic Holocene tephra in Iceland and Scotland. J. Quat. Sci. 7, 173–183.

Dugmore, A.J., Larsen, G., Newton, A.J., 1995. Seven tephra isochrones in Scotland. Holocene 5, 257–266.

Dunbar, N.W., Iverson, N.A., Van Eaton, A.R., Sigl, M., Alloway, B.V., Kurbatov, A.V., Mastin, L.G., McConnell, J.R., Wilson, C.J., 2017. New Zealand supereruption provides time marker for the Last Glacial Maximum in Antarctica. Sci. Rep. 7, 12238.

Faral, A., Lavigne, F., Mutaqin, B.W., Mokadem, F., Achmad, R., Ningrum, R.W., Lahitte, P., Hadmoko, D.S., Mei, E.T.W., 2022. A 22,000-year tephrostratigraphy record of unidentified volcanic eruptions from Ternate and Tidore islands (North Maluku, Indonesia). J. Volcanol. Geoth. Res. 423, 107474.

Fiacco Jr., R.J., Palais, J.M., Germani, M.S., Zielinski, G.A., Mayewski, P.A., 1993. Characteristics and possible source of a 1479 AD volcanic ash layer in a Greenland ice core. Quat. Res. 39, 267–273.

Fiacco Jr., R.J., Thordarson, T., Germani, M.S., Self, S., Palais, J.M., Whitlow, S., Grootes, P.M., 1994. Atmospheric aerosol loading and transport due to the 1783-84 Laki eruption in Iceland, interpreted from ash particles and acidity in the GISP2 ice core. Quat. Res. 42, 231–240.

Fischer, E.M., Luterbacher, J., Zorita, E., Tett, S.F.B., Casty, C., Wanner, H., 2007. European climate response to tropical volcanic eruptions over the last half

millennium. Geophys. Res. Lett. 34, L05707.
Fyfe, R.M., Blackford, J.J., Hardiman, M., Hazell, Z., MacLeod, A., Perez, M., Littlewood, S., 2016. The environment of the Whitehorse Hill cist. In: Jones, A.M. (Ed.), Preserved in the Peat: an Extraordinary Bronze Age Burial on Whitehorse Hill, Dartmoor, and its Wider Context. Oxbow, Oxford, pp. 158–181.
Garrison, C.S., Kilburn, C.R., Edwards, S.J., 2018. The 1831 eruption of Babuyan Claro that never happened: has the source of one of the largest volcanic climate forcing events of the nineteenth century been misattributed? J. Appl. Volcanol. 7, 8.
Garrison, C., Kilburn, C., Smart, D., Edwards, S., 2021. The blue suns of 1831: was the eruption of Ferdinandea, near Sicily, one of the largest volcanic climate forcing events of the nineteenth century? Climate Past 17, 2607–2632.
Gautier, E., Savarino, J., Hoek, J., Erbland, J., Caillon, N., Hattori, S., Yoshida, N., Albalat, E., Albarede, F., Farquhar, J., 2019. 2600-years of stratospheric volcanism through sulfate isotopes. Nature Commun. 10, 466.
Gjerløw, E., Höskuldsson, A., Pedersen, R.B., 2015. The 1732 Surtseyan eruption of Eggøya, Jan Mayen, North Atlantic: deposits, distribution, chemistry and chronology. Bull. Volcanol. 77, 14.
Gregory, J.M., Andrews, T., Good, P., Mauritsen, T., Forster, P.M., 2016. Small global-mean cooling due to volcanic radiative forcing. Clim. Dynam. 47, 3979–3991.
Grönvold, K., Óskarsson, N., Johnsen, S.J., Clausen, H.B., Hammer, C.U., Bond, G., Bard, E., 1995. Ash layers from Iceland in the Greenland GRIP ice core correlated with oceanic and land sediments. Earth Planet. Sci. Lett. 135, 145–155.
Gudmundsdóttir, E.R., Larsen, G., Eiríksson, J., 2012. Tephra stratigraphy on the North Icelandic shelf: extending tephrochronology into marine sediments off North Iceland. Boreas 41, 719–734.
Gudmundsdóttir, E.R., Larsen, G., Björck, S., Ingólfsson, Ó., Striberger, J., 2016. A new high-resolution Holocene tephra stratigraphy in eastern Iceland: improving the Icelandic and North Atlantic tephrochronology. Quat. Sci. Rev. 150, 234–249.
Gudmundsdóttir, E.R., Schomacker, A., Brynjólfsson, S., Ingólfsson, Ó., Larsen, N.K., 2018. Holocene tephrostratigraphy in Vestfirðir, NW Iceland. J. Quat. Sci. 33, 827–839.
Guillet, S., Corona, C., Stoffel, M., Khodri, M., Lavigne, F., Ortega, P., Eckert, N., Sielenou, P.D., Daux, V., Davi, N., Edouard, J.L., 2017. Climate response to the Samalas volcanic eruption in 1257 revealed by proxy records. Nat. Geosci. 10, 123–128.
Guillet, S., Corona, C., Ludlow, F., Oppenheimer, C., Stoffel, M., 2020. Climatic and societal impacts of a "forgotten" cluster of volcanic eruptions in 1108-1110 CE. Sci. Rep. 10, 6715.
Gutiérrez, X., Schiavi, F., Keppler, H., 2016. The adsorption of HCl on volcanic ash. Earth Planet Sci. Lett. 438, 66–74.
Haflidason, H., Eiriksson, J., van Kreveld, S., 2000. The tephrochronology of Iceland and the North Atlantic region during the Middle and Late Quaternary: a review. J. Quat. Sci. 15, 3–22.
Hall, V.A., Pilcher, J.R., 2002. Late-Quaternary Icelandic tephras in Ireland and Great Britain: detection, characterization and usefulness. Holocene 12, 223–230.
Hannon, G.E., Hermanns-Audardóttir, M., Wastegård, S., 1998. Human impact at Tjørnuvík in the Faroe Islands. Fróðskaparrit 46, 215–228.
Hammer, C.U., Kurat, G., Hoppe, P., Grum, W., Clausen, H.B., 2003. Thera eruption date 1645BC confirmed by new ice core data? In: Bietak, M. (Ed.), The Synchronisation of Civilisations in the Eastern Mediterranean in the Second Millennium B.C. Proceedings of the SCIEM 2000 - EuroConference Haindorf, May 2001. Verlag der Osterreichischen Akademie der Wissenschaften, Vienna. Band XXIX, pp. 87–93.
Hasegawa, T., Nakagawa, M., Yoshimoto, M., Ishizuka, Y., Hirose, W., Seki, S.I., Ponomareva, V., Alexander, R., 2011. Tephrostratigraphy and petrological study of Chikurachki and Fuss volcanoes, western Paramushir Island, northern Kurile Islands: evaluation of Holocene eruptive activity and temporal change of magma system. Quat. Int. 246, 278–297.
Iverson, N.A., Kalteyer, D., Dunbar, N.W., Kurbatov, A., Yates, M., 2017. Advancements and best practices for analysis and correlation of tephra and cryptotephra in ice. Quat. Geochronol. 40, 45–55.
Jennings, A., Thordarson, T., Zalzal, K., Stoner, J., Hayward, C., Geirsdóttir, Á., Miller, G., 2014. Holocene tephra from Iceland and Alaska in SE Greenland shelf sediments. Geological Society, London, Special Publications 398, 157–193.
Jensen, B., Pyne-O'Donnell, S., Plunkett, G., Froese, D.G., Hughes, P.D.M., Sigl, M., McConnell, J.R., Amesbury, M.J., Blackwell, P.G., van den Bogaard, C., Buck, C.E., Charman, D.J., Clague, J.J., Hall, V., Koch, J., Mackay, H., Mallon, G., McColl, L., Pilcher, J.R., 2014. Transatlantic distribution of the Alaskan White River Ash. Geology 42, 875–878.
Jensen, B.J., Davies, L.J., Nolan, C., Pyne-O'Donnell, S., Monteath, A.J., Ponomareva, V., Portnyagin, M., Booth, R., Bursik, M., Cook, E., Plunkett, G., Vallance, J.W., Luo, Y., Cwynar, L.C., Hughes, P., Pearson, D.G., 2021. A latest Pleistocene and Holocene composite tephrostratigraphic framework for northeastern North America. Quat. Sci. Rev. 272, 107242.
Johansson, H., Lind, E.M., Wastegård, S., 2017. Compositions of glass in proximal tephras from eruptions in the Azores archipelago and their links with distal sites in Ireland. Quat. Geochronol. 40, 120–128.
Jones, G., Davies, S.M., Staff, R.A., Loader, N.J., Davies, S.J., Walker, M.J., 2020. Traces of volcanic ash from the Mediterranean, Iceland and North America in a Holocene record from south Wales, UK. J. Quat. Sci. 35, 163–174.
Jónsson, D.F., Gudmundsdóttir, E.R., Larsen, G., Óladóttir, B.A., Erlendsson, E., Eddudóttir, S.D., Sigmarsson, O., 2020. The multi-component Hekla Ó Tephra, Iceland: a complex widespread mid-Holocene tephra layer. J. Quat. Sci. 35, 410–421.
Jungclaus, J.H., Bard, E., Baroni, M., Braconnot, P., Cao, J., Chini, L.P., Egorova, T., Evans, M., González-Rouco, J.F., Goosse, H., Hurtt, G.C., Joos, F., Kaplan, J.O., Khodri, M., Klein Goldewijk, K., Krivova, N., LeGrande, A.N., Lorenz, S.J., Luterbacher, J., Man, W., Maycock, A.C., Meinshausen, M., Moberg, A., Muscheler, R., Nehrbass-Ahles, C., Otto-Bliesner, B.I., Phipps, S.J., Pongratz, J., Rozanov, E., Schmidt, G.A., Schmidt, H., Schmutz, W., Schurer, A., Shapiro, A.I., Sigl, M., Smerdon, J.E., Solanki, S.K., Timmreck, C., Toohey, M., Usoskin, I.G., Wagner, S., Wu, C.-J., Yeo, K.L., Zanchettin, D., Zhang, Q., Zorita, E., 2017. The PMIP4 contribution to CMIP6–Part 3: the last millennium, scientific objective, and experimental design for the PMIP4 past1000 simulations. Geosci. Model Dev. (GMD) 10, 4005–4033.
Kalliokoski, M., Wastegård, S., Saarinen, T., 2019. Rhyolitic and dacitic component of the Askja 1875 tephra in southern and central Finland: first step towards a Finnish tephrochronology. J. Quat. Sci. 34, 29–39.
Kalliokoski, M., Guðmundsdóttir, E.R., Wastegård, S., 2020. Hekla 1947, 1845, 1510 and 1158 tephra in Finland: challenges of tracing tephra from moderate eruptions. J. Quat. Sci. 35, 803–816.
Kinder, M., Wulf, S., Appelt, O., Hardiman, M., Żarczyński, M., Tylmann, W., 2020. Late-Holocene ultra-distal cryptotephra discoveries in varved sediments of Lake Żabińskie, NE Poland. J. Volcanol. Geoth. Res. 402, 106988.
Kinder, M., Wulf, S., Appelt, O., 2021. Detection of the historical Askja AD 1875 and modern Icelandic cryptotephras in varved lake sediments–results from a first systematic search in northern Poland. J. Quat. Sci. 36, 1–7.
Kobashi, T., Menviel, L., Jeltsch-Thömmes, A., Vinther, B.M., Box, J.E., Muscheler, R., Nakaegawa, T., Pfister, P.L., Döring, M., Leuenberger, M., Wanner, H., Ohmura, A., 2017. Volcanic influence on centennial to millennial Holocene Greenland temperature change. Sci. Rep. 7, 1–10.
Koren, J.H., Svendsen, J.I., Mangerud, J., Furnes, H., 2008. The Dimna Ash—a 12.8 ^{14}C ka-old volcanic ash in Western Norway. Quat. Sci. Rev. 27, 85–94.
Krasheninnikov, S.P., Bazanova, L.I., Ponomareva, V.V., Portnyagin, M.V., 2020. Detailed tephrochronology and composition of major Holocene eruptions from Avachinsky, Kozelsky, and Koryaksky volcanoes in Kamchatka. J. Volcanol. Geoth. Res. 408, 107088.
Kremser, S., Thomason, L.W., von Hobe, M., Hermann, M., Deshler, T., Timmreck, C., Toohey, M., Stenke, A., Schwarz, J.P., Weigel, R., Fueglistaler, S., Prata, F.J., Vernier, J.-P., Schlager, H., Barnes, J.E., Antuña-Marrero, J.-C., Fairlie, D., Palm, M., Mahieu, E., Notholt, J., Rex, M., Bingen, C., Vanhellemont, F., Bourassa, A., Plane, J.M.C., Klocke, D., Carn, S.A., Clarisse, L., Trickl, T., Neely, R., James, A.D., Rieger, L., Wilson, J.C., Meland, B., 2016. Stratospheric aerosol—observations, processes, and impact on climate. Rev. Geophys. 54, 278–335.
Kurbatov, A.V., Zielinski, G.A., Dunbar, N.W., Mayewski, P.A., Meyerson, E.A., Sneed, S.B., Taylor, K.C., 2006. A 12,000 year record of explosive volcanism in the Siple Dome ice core, west Antarctica. J. Geophys. Res.: Atmos. 111, D12307.
LaMarche Jr., V.C., Hirschboeck, K.K., 1984. Frost rings in trees as records of major volcanic eruptions. Nature 307, 121–126.
Langway Jr., C.C., Osada, K., Clausen, H.B., Hammer, C.U., Shoji, H., 1995. A 10-century comparison of prominent bipolar volcanic events in ice cores. J. Geophys. Res.: Atmos. 100 (D8), 16241–16247.
Larsen, G., 1984. Recent volcanic history of the Veidivötn fissure swarm, southern Iceland — an approach to volcanic risk assessment. J. Volcanol. Geoth. Res. 22, 33–58.
Larsen, G., Dugmore, A.J., Newton, A.J., 1999. Geochemistry of historic silicic tephras in Iceland. Holocene 9, 463–471.
Larsen, G., Newton, A.J., Dugmore, A.J., Vilmundardóttir, E.G., 2001. Geochemistry, dispersal, volumes and chronology of Holocene silicic tephra layers from the Katla volcanic system, Iceland. J. Quat. Sci. 16, 119–132.
Larsen, J.F., Nye, C.J., Coombs, M.L., Tilman, M., Izbekov, P., Cameron, C., 2010. Petrology and geochemistry of the 2006 eruption of augustine volcano. In: Power, J.A., Coombs, M.L., Freymueller, J.T. (Eds.), The 2006 Eruption of Augustine Volcano, Alaska. US Geological Survey Professional Paper No. 1769-15, pp. 335–382.
Lavigne, F., Degeai, J.P., Komorowski, J.C., Guillet, S., Robert, V., Lahitte, P., Oppenheimer, C., Stoffel, M., Vidal, C.M., Surono I., Pratomo, Wassmera, P., Hajdask, I., Hadmokol, D.S., de Belizala, E., 2013. Source of the great AD 1257 mystery eruption unveiled, Samalas volcano, Rinjani Volcanic Complex, Indonesia. Proc. Natl. Acad. Sci. USA 110, 16742–16747.
Le Bas, M.J., Le Maitre, R.W., Streckeisen, A., Zanettin, B., 1986. A chemical classification of volcanic rocks on the total alkali–silica diagram. J. Petrol. 27, 745–750.
LeGrande, A.N., Tsigaridis, K., Bauer, S.E., 2016. Role of atmospheric chemistry in the climate impacts of stratospheric volcanic injections. Nat. Geosci. 9, 652–655.
Li, Y.C., 2013. The textual research on the Wangtian'e volcano eruption on October 6, 1597. Seismol. Ecol. 35, 315–321.
Longpré, M.A., Klügel, A., Diehl, A., Stix, J., 2014. Mixing in mantle magma reservoirs prior to and during the 2011–2012 eruption at El Hierro, Canary Islands. Geology 42, 315–318.
Mackay, H., Hughes, P.D.M., Jensen, B.J.L., Langdon, P.G., Pyne-O'Donnell, S.D.F., Plunkett, G., Froese, D.G., Coulter, S., Gardner, J., 2016. A mid to late Holocene cryptotephra framework from eastern North America. Quat. Sci. Rev. 132, 101–113.
Mackay, H., Plunkett, G., Jensen, B.J.L., Aubry, T.J., Corona, C., Kim, W.M., Toohey, M., Sigl, M., Stoffel, M., Anchukaitis, K.J., Raible, C., Bolton, M.S.M., Manning, J.G., Newfield, T.P., Di Cosmo, N., Ludlow, F., Kostick, C., Yang, Z., Coyle McClung, L., Amesbury, M., Monteath, A., Hughes, P.D.M., Langdon, P.G., Charman, D., Booth, R., Davies, K.L., Blundell, A., Swindles, G.T., 2022. The 852/3 CE mount Churchill eruption: examining the potential climatic and societal impacts and

the timing of the medieval climate anomaly in the North Atlantic region. Climate Past 18, 1475–1508.
Malavelle, F.F., Haywood, J.M., Jones, A., Gettelman, A., Clarisse, L., Bauduin, S., Allan, R.P., Karset, I.H.H., Kristjánsson, J.E., Oreopoulos, L., Cho, N., Lee, D., Bellouin, N., Boucher, O., Grosvenor, D.P., Carslaw, K.S., Dhomse, S., Mann, G.W., Schmidt, A., Coe, H., Hartley, M.E., Dalvi, M., Hill, A.A., Johnson, B.T., Johnson, C.E., Knight, J.R., O'Connor, F.M., Partridge, D.G., Stier, P., Myhre, G., Platnick, S., Stephens, G.L., Takahashi, H., Thordarson, T., 2017. Strong constraints on aerosol–cloud interactions from volcanic eruptions. Nature 546, 485–491.
Mandeville, C.W., Carey, S., Sigurdsson, H., 1996. Magma mixing, fractional crystallization and volatile degassing during the 1883 eruption of Krakatau volcano, Indonesia. J. Volcanol. Geoth. Res. 74, 243–274.
Mangerud, J., Lie, S.E., Furnes, H., Kristiansen, I.L., Lømo, L., 1984. A Younger Dryas ash bed in western Norway, and its possible correlations with tephra in cores from the Norwegian Sea and the North Atlantic. Quat. Res. 21, 85–104.
Marcaida, M., Mangan, M.T., Vazquez, J.A., Bursik, M., Lidzbarski, M.I., 2014. Geochemical fingerprinting of Wilson Creek formation tephra layers (Mono Basin, California) using titanomagnetite compositions. J. Volcanol. Geoth. Res. 273, 1–14.
Marshall, L., Johnson, J.S., Mann, G.W., Lee, L., Dhomse, S.S., Regayre, L., Yoshioka, M., Carslaw, K.S., Schmidt, A., 2019. Exploring how eruption source parameters affect volcanic radiative forcing using statistical emulation. J. Geophys. Res.: Atmos. 124, 964–985.
Marshall, L.R., Smith, C.J., Forster, P.M., Aubry, T.J., Andrews, T., Schmidt, A., 2020. Large variations in volcanic aerosol forcing efficiency due to eruption source parameters and rapid adjustments. Geophys. Res. Lett. 47, e2020GL090241.
Marshall, L.R., Schmidt, A., Johnson, J.S., Mann, G.W., Lee, L.A., Rigby, R., Carslaw, K.S., 2021. Unknown eruption source parameters cause large uncertainty in historical volcanic radiative forcing reconstructions. J. Geophys. Res.: Atmos. 126, e2020JD033578.
Martí, J., Castro, A., Rodríguez, C., Costa, F., Carrasquilla, S., Pedreira, R., Bolos, X., 2013. Correlation of magma evolution and geophysical monitoring during the 2011–2012 El Hierro (Canary Islands) submarine eruption. J. Petrol. 54, 1349–1373.
Martin-Puertas, C., Walsh, A.A., Blockley, S.P., Harding, P., Biddulph, G.E., Palmer, A., Ramisch, A., Brauer, A., 2021. The first Holocene varve chronology for the UK: based on the integration of varve counting, radiocarbon dating and tephrostratigraphy from Diss Mere (UK). Quat. Geochronol. 61, 101134.
McConnell, J.R., 2013. Microparticle and Trace Element Studies, In S.A. Elias, C.J. Mock (Eds), Encyclopedia Quat. Sci. (second edition), pp. 342–346.
McConnell, J.R., Burke, A., Dunbar, N.W., Köhler, P., Thomas, J.L., Arienzo, M.M., Chellman, N.J., Maselli, O.J., Sigl, M., Adkins, J.F., Baggenstos, D., 2017. Synchronous volcanic eruptions and abrupt climate change~ 17.7 ka plausibly linked by stratospheric ozone depletion. Proc. Nat. Acad. Sci. USA 114, 10035–10040.
McConnell, J.R., Wilson, A.I., Stohl, A., Arienzo, M.M., Chellman, N.J., Eckhardt, S., Thompson, E.M., Pollard, A.M., Steffensen, J.P., 2018. Lead pollution recorded in Greenland ice indicates European emissions tracked plagues, wars, & imperial expansion during antiquity. Proc. Nat. Acad. Sci. USA 115, 5726–5731.
McConnell, J.R., Sigl, M., Plunkett, G., Burke, A., Wilson, A.J., Manning, J., Ludlow, F., Chellman, N.J., Innes, H.M., Larsen, J.F., Schaefer, J.R., Kipfstuhl, S., Mojtabavi, S., Whilhelms, F., Opel, T., Meyer, H., Steffensen, J.P., 2020. Extreme climate after massive eruption of Alaska's Okmok volcano in 43 BCE and effects on the late Roman Republic and Ptolemaic Kingdom. Proc. Nat. Acad. Sci. USA 117, 15443–15449.
Miller, G.H., Geirsdóttir, Á., Zhong, Y., Larsen, D.L., Otto-Bliesner, B.L., Holland, M.M., Bailey, D.A., Refsnider, K.A., Lehman, S.J., Southon, J.R., Anderson, C., Björnsson, H., Thordarson, T., 2012. Abrupt onset of the Little Ice Age triggered by volcanism and sustained by sea-ice/ocean feedbacks. Geophys. Res. Lett. 39, L02708.
Moles, J.D., McGarvie, D., Stevenson, J.A., Sherlock, S.C., Abbott, P.M., Jenner, F.E., Halton, A.M., 2019. Widespread tephra dispersal and ignimbrite emplacement from a subglacial volcano (Torfajökull, Iceland). Geology 47, 577–580.
Moreland, W.M., Thordarson, T., Houghton, B.F., Larsen, G., 2019. Driving mechanisms of subaerial and subglacial explosive episodes during the 10th century Eldgjá fissure eruption, southern Iceland. Volcanica 2, 129–150.
Narcisi, B., Petit, J.R., Delmonte, B., Batanova, V., Savarino, J., 2019. Multiple sources for tephra from AD 1259 volcanic signal in Antarctic ice cores. Quat. Sci. Rev. 210, 164–174.
Niemeier, U., Timmreck, C., Graf, H.F., Kinne, S., Rast, S., Self, S., 2009. Initial fate of fine ash and sulfur from large volcanic eruptions. Atmos. Chem. Phys. 9, 9043–9057.
Óladóttir, B.A., Larsen, G., Thordarson, T., Sigmarsson, O., 2005. The Katla volcano S-Iceland: Holocene tephra stratigraphy and eruption frequency. Jökull 55, 53–74.
Óladóttir, B.A., Sigmarsson, O., Larsen, G., Thordarson, T., 2008. Katla volcano, Iceland: magma composition, dynamics and eruption frequency as recorded by Holocene tephra layers. Bull. Volcanol. 70, 475–493.
Óladóttir, B.A., Larsen, G., Sigmarsson, O., 2011. Holocene volcanic activity at Grímsvötn, Bárdarbunga and Kverkfjöll subglacial centres beneath Vatnajökull, Iceland. Bull. Volcanol. 73, 1187–1208.
Óladóttir, B.A., Larsen, G., Sigmarsson, O., 2014. Volume estimates of nine Katla tephra layers (~ 1860 BC–870 AD). Jökull 64, 23–40.
Oppenheimer, C., Wacker, L., Xu, J., Galván, J.D., Stoffel, M., Guillet, S., Corona, C., Sigl, M., Di Cosmo, N., Hajdas, I., Pan, B., Breuker, R., Schneider, L., Esper, J., Fei, J., Hammond, J.O.S., Büntgen, U., 2017. Multi-proxy dating the 'Millennium Eruption' of Changbaishan to late 946 CE. Quat. Sci. Rev. 158, 164–171.
Oppenheimer, C., Orchard, A., Stoffel, M., Newfield, T.P., Guillet, S., Corona, C., Sigl, M., Di Cosmo, N., Büntgen, U., 2018. The Eldgjá eruption: timing, long-range impacts and influence on the Christianisation of Iceland. Climatic Change 147, 369–381.
Otto-Bliesner, B.L., Brady, E.C., Fasullo, J., Jahn, A., Landrum, L., Stevenson, S., Rosenbloom, N., Mai, A., Strand, G., 2016. Climate variability and change since 850 CE: an ensemble approach with the community Earth system model. Bull. Am. Meteorol. Soc. 97, 735–754.
Palais, J.M., Kirchner, S., Delmas, R.J., 1990. Identification of some global volcanic horizons by major element analysis of fine ash in Antarctic ice. Ann. Glaciol. 14, 216–220.
Palais, J.M., Taylor, K., Mayewski, P.A., Grootes, P., 1991. Volcanic ash from the 1362 A.D. Oræfajokull eruption (Iceland) in the Greenland ice sheet. Geophys. Res. Lett. 18, 1241–1244.
Palais, J.M., Germani, M.S., Zielinski, G.A., 1992. Inter-hemispheric transport of volcanic ash from a 1259 AD volcanic eruption to the Greenland and Antarctic ice sheets. Geophys. Res. Lett. 19, 801–804.
Pearce, N.J.G., Westgate, J.A., Preece, S.J., Eastwood, W.J., Perkins, W.T., 2004a. Identification of Aniakchak (Alaska) tephra in Greenland ice core challenges the 1645 BC date for Minoan eruption of Santorini. G-cubed 5, Q03005.
Pearce, N.J., Westgate, J.A., Perkins, W.T., Preece, S.J., 2004b. The application of ICP-MS methods to tephrochronological problems. Appl. Geochem. 19, 289–322.
Pearson, C., Sigl, M., Burke, A., Davies, S., Kurbatov, A., Severi, M., Cole-Dai, J., Innes, H., Albert, P.G., Helmick, M., 2022. Geochemical ice-core constraints on the timing and climatic impact of Aniakchak II (1628 BCE) and Thera (Minoan) volcanic eruptions. PNAS Nexus 1, pgac048.
Pilcher, J.R., Hall, V.A., McCormac, F.G., 1995. Dates of Holocene Icelandic volcanic eruptions from tephra layers in Irish peats. Holocene 5, 103–110.
Pilcher, J.R., Hall, V.A., McCormac, F.G., 1996. An outline tephrochronology for the Holocene of the north of Ireland. J. Quat. Sci. 11, 485–494.
Pilcher, J., Bradley, R.S., Francus, P., Anderson, L., 2005. A Holocene tephra record from the Lofoten Islands, arctic Norway. Boreas 34, 136–156.
Pinto, J.P., Turco, R.P., Toon, O.B., 1989. Self-limiting physical and chemical effects in volcanic eruption clouds. J. Geophys. Res.: Atmos. 94 (D8), 11165–11174.
Plummer, C.T., Curran, M.A., van Ommen, T.D., Rasmussen, S.O., Moy, A.D., Vance, T.R., Clausen, H.B., Vinther, B.M., Mayewski, P.A., 2012. An independently dated 2000-yr volcanic record from Law Dome, East Antarctica, including a new perspective on the dating of the 1450s CE eruption of Kuwae, Vanuatu. Climate Past 8, 1929–1940.
Plunkett, G., Pilcher, J.R., 2018. Defining the potential sources region of volcanic ash in northwest Europe during the Mid- to Late Holocene. Earth Sci. Rev. 179, 20–37.
Plunkett, G., Pearce, N.J., McConnell, J., Pilcher, J., Sigl, M., Zhao, H., 2017. Trace element analysis of Late Holocene tephras from Greenland ice cores. Quat. Newsl. 143, 10–21.
Plunkett, G., Sigl, M., Pilcher, J.R., McConnell, J.R., Chellman, N., Steffensen, J.P., Büntgen, U., 2020. Smoking guns and volcanic ash: the importance of sparse tephras in Greenland ice cores. Polar Res. 39, 3511.
Plunkett, G., Sigl, M., Schwaiger, H., Tomlinson, E., Toohey, M., McConnell, J.R., Pilcher, J.R., Hasegawa, T., Siebe, C., 2022. No evidence for tephra in Greenland from the historic eruption of Vesuvius in 79 CE: implications for geochronology and paleoclimatology. Climate Past 18, 45–65.
Ponomareva, V., Portnyagin, M., Pevzner, M., Blaauw, M., Kyle, P., Derkachev, A., 2015. Tephra from andesitic Shiveluch volcano, Kamchatka, NW Pacific: chronology of explosive eruptions and geochemical fingerprinting of volcanic glass. Int. J. Earth Sci. 104, 1459–1482.
Portnyagin, M.V., Ponomareva, V.V., Zelenin, E.A., Bazanova, L.I., Pevzner, M.M., Plechova, A.A., Rogozin, A.N., Garbe-Schönberg, D., 2020. TephraKam: geochemical database of glass compositions in tephra and welded tuffs from the Kamchatka volcanic arc (northwestern Pacific). Earth Syst. Sci. Data 12, 469–486.
Prata, F., Woodhouse, M., Huppert, H.E., Prata, A., Thordarson, T., Carn, S., 2017. Atmospheric processes affecting the separation of volcanic ash and SO_2 in volcanic eruptions: inferences from the May 2011 Grímsvötn eruption. Atmos. Chem. Phys. 17, 10709–10732.
Pueschel, R.F., Russell, P.B., Allen, D.A., Ferry, G.V., Snetsinger, K.G., Livingston, J.M., Verma, S., 1994. Physical and optical properties of the Pinatubo volcanic aerosol: aircraft observations with impactors and a Sun-tracking photometer. J. Geophys. Res.: Atmos. 99 (D6), 12915–12922.
Robock, A., 2000. Volcanic eruptions and climate. Rev. Geophys. 38, 191–219.
Rose, W.I., Bluth, G.J., Schneider, D.J., Ernst, G.G., Riley, C.M., Henderson, L.J., McGimsey, R.G., 2001. Observations of volcanic clouds in their first few days of atmospheric residence: the 1992 eruptions of Crater Peak, Mount Spurr Volcano, Alaska. J. Geol. 109, 677–694.
Schmid, M.M., Dugmore, A.J., Vésteinsson, O., Newton, A.J., 2017. Tephra isochrons and chronologies of colonisation. Quat. Geochronol. 40, 56–66.
Schmidt, A., Carslaw, K.S., Mann, G.W., Rap, A., Pringle, K.J., Spracklen, D.V., Wilson, M., Forster, P.M., 2012. Importance of tropospheric volcanic aerosol for indirect radiative forcing of climate. Atmos. Chem. Phys. 12, 7321–7339.
Schmidt, A., Mills, M.J., Ghan, S., Gregory, J.M., Allan, R.P., Andrews, T., Bardeen, C.G., Conley, A., Forster, P.M., Gettelman, A., Portmann, R.W., 2018. Volcanic radiative forcing from 1979 to 2015. J. Geophys. Res.: Atmos. 123, 12491–12508.
Schurer, A.P., Hegerl, G.C., Mann, M.E., Tett, S.F., Phipps, S.J., 2013. Separating forced

from chaotic climate variability over the past millennium. J. Clim. 26, 6954–6973.
Shinohara, H., 2008. Excess degassing from volcanoes and its role on eruptive and intrusive activity. Rev. Geophys. 46, RG4005.
Siebert, L., Simkin, T., Kimberly, P., 2010. Volcanoes of the World, third ed. University of California Press, Berkeley.
Sigl, M., McConnell, J.R., Layman, L., Maselli, O., McGwire, K., Pasteris, D., Dahl-Jensen, D., Steffensen, J.P., Vinther, B., Edwards, R., Mulvaney, R., 2013. A new bipolar ice core record of volcanism from WAIS Divide and NEEM and implications for climate forcing of the last 2000 years. J. Geophys. Res.: Atmos. 118, 1151–1169.
Sigl, M., Winstrup, M., McConnell, J.R., Welten, K.C., Plunkett, G., Ludlow, F., Büntgen, U., Caffee, M., Chellman, N., Dahl-Jensen, D., Fischer, H., Kipfstuhl, S., Kostick, C., Maselli, O.J., Mekhaldi, F., Mulvaney, R., Muscheler, R., Pasteris, D.R., Pilcher, J.R., Salzer, M., Schüpbach, S., Steffensen, J.P., Vinther, B.M., Woodruff, T.E., 2015. Timing and climate forcing of volcanic eruptions for the past 2,500 years. Nature 523, 543–549.
Sigl, M., Toohey, M., McConnell, J.R., Cole-Dai, J., Severi, M., 2022. Volcanic stratospheric sulfur injections and aerosol optical depth during the Holocene (past 11,500 years) from a bipolar ice core array. Earth Syst. Sci. Data 14, 3167–3196.
Sigurgeirsson, M.Á., Hauptfleisch, U., Newton, A., Einarsson, Á., 2013. Dating of the Viking age Landnám tephra sequence in Lake Mývatn sediment, north Iceland. J. North Atlantic 21, 1–11.
Sinnl, G., Winstrup, M., Erhardt, T., Cook, E., Jensen, C.M., Svensson, A., Vinther, B.M., Muscheler, R., Rasmussen, S.O., 2022. A multi-ice-core, annual-layer-counted Greenland ice-core chronology for the last 3800 years: GICC21. Climate Past 18, 1125–1150.
Smith, V.C., Costa, A., Aguirre-Díaz, G., Pedrazzi, D., Scifo, A., Plunkett, G., Poret, M., Tournigand, P.Y., Miles, D., Dee, M.W., McConnell, J.R., Suñe-Puchol, I., Dávila Harris, P., Sigl, M., Pilcher, J.R., Chellman, N., Gutiérrez, E., 2020. The timing and impact of the large Tierra Blanca Joven eruption of Ilopango, El Salvador. Proc. Nat. Acad. Sci. USA 117, 26061–26068.
Smith, V.C., Staff, R.A., Blockley, S.P., Ramsey, C.B., Nakagawa, T., Mark, D.F., Takemura, K., Danhara, T., Suigetsu 2006 Project Members, 2013. Identification and correlation of visible tephras in the Lake Suigetsu SG06 sedimentary archive, Japan: chronostratigraphic markers for synchronising of east Asian/west Pacific palaeoclimatic records across the last 150 ka. Quat. Sci. Rev. 67, 121–137.
Staunton-Sykes, J., Aubry, T.J., Shin, Y.M., Weber, J., Marshall, L.R., Luke Abraham, N., Archibald, A., Schmidt, A., 2021. Co-emission of volcanic sulfur and halogens amplifies volcanic effective radiative forcing. Atmos. Chem. Phys. 21, 9009–9029.
Stevenson, J.A., Loughlin, S.C., Font, A., Fuller, G.W., MacLeod, A., Oliver, I.W., Jackson, B., Horwell, C.J., Thordarson, T., Dawson, I., 2013. UK monitoring and deposition of tephra from the May 2011 eruption of Grímsvötn, Iceland. J. Appl. Volcanol. 2, 3.
Stocker, M., Ladstädter, F., Wilhelmsen, H., Steiner, A.K., 2019. Quantifying stratospheric temperature signals and climate imprints from post-2000 volcanic eruptions. Geophys. Res. Lett. 46, 12486–12494.
Stoffel, M., Corona, C., Ludlow, F., Sigl, M., Huhtamaa, H., Garnier, E., Helama, S., Guillet, S., Crampsie, A., Kleemann, K., Camenisch, C., 2022. Climatic, weather, and socio-economic conditions corresponding to the mid-17th-century eruption cluster. Climate Past 18, 1083–1108.
Sun, C., Plunkett, G., Liu, J., Zhao, H., Sigl, M., McConnell, J.R., Pilcher, J.R., Vinther, B., Steffensen, J.P., Hall, V., 2014. Ash from Changbaishan Millennium eruption recorded in Greenland ice: implications for determining the eruption's timing and impact. Geophys. Res. Lett. 41, 694–701.
Sun, C., Wang, L., Plunkett, G., You, H., Zhu, Z., Zhang, L., Zhang, B., Chu, G., Liu, J., 2018. Ash from the Changbaishan Qixiangzhan eruption: a new early Holocene marker horizon across east Asia. J. Geophys. Res.: Solid Earth 123, 6442–6450.
Swingedouw, D., Mignot, J., Ortega, P., Khodri, M., Menegoz, M., Cassou, C., Hanquiez, V., 2017. Impact of explosive volcanic eruptions on the main climate variability modes. Global Planet. Change 150, 24–45.
Thomason, L.W., Ernest, N., Millán, L., Rieger, L., Bourassa, A., Vernier, J.P., Manney, G., Luo, B., Arfeuille, F., Peter, T., 2018. A global space-based stratospheric aerosol climatology: 1979–2016. Earth Syst. Sci. Data 10, 469–492.
Thordarson, T., Höskuldsson, Á., 2008. Postglacial volcanism in Iceland. Jökull 588, 197–228.
Thordarson, T., Self, S., 2003. Atmospheric and environmental effects of the 1783–1784 Laki eruption: a review and reassessment. J. Geophys. Res.: Atmos. 108 (D1), 4011.
Thordarson, T., Self, S., Oskarsson, N., Hulsebosch, T., 1996. Sulfur, chlorine, and fluorine degassing and atmospheric loading by the 1783–1784 AD Laki (Skaftár Fires) eruption in Iceland. Bull. Volcanol. 58, 205–225.
Thordarson, T., Miller, D.J., Larsen, G., Self, S., Sigurdsson, H., 2001. New estimates of sulfur degassing and atmospheric mass-loading by the 934 AD Eldgjá eruption, Iceland. J. Volcanol. Geoth. Res. 108, 33–54.
Timmreck, C., 2012. Modeling the climatic effects of large explosive volcanic eruptions. WIRES: Clim. Change 3, 545–564.
Timmreck, C., Mann, G.W., Aquila, V., Hommel, R., Lee, L.A., Schmidt, A., Brühl, C., Carn, S., Chin, M., Dhomse, S.S., English, J.M., Mills, M.J., Neely, R., Sheng, J., Toohey, M., Weisenstein, D., 2018. The interactive stratospheric aerosol model intercomparison project (ISA-MIP): motivation and experimental design. Geosci. Model Dev. (GMD) 11, 2581–2608.
Timmreck, C., Toohey, M., Zanchettin, D., Brönnimann, S., Lundstad, E., Wilson, R., 2021. The unidentified eruption of 1809: a climatic cold case. Climate Past 17, 1455–1482.
Tomlinson, E.L., Smith, V.C., Albert, P.G., Aydar, E., Civetta, L., Cioni, R., Çubukçu, E., Gertisser, R., Isaia, R., Menzies, M.A., Orsi, G., 2015. The major and trace element glass compositions of the productive Mediterranean volcanic sources: tools for correlating distal tephra layers in and around Europe. Quat. Sci. Rev. 118, 48–66.
Toohey, M., Sigl, M., 2017. Volcanic stratospheric sulfur injections and aerosol optical depth from 500 BCE to 1900 CE. Earth Syst. Sci. Data 9, 809–831.
Toohey, M., Krüger, K., Timmreck, C., 2013. Volcanic sulfate deposition to Greenland and Antarctica: a modeling sensitivity study. J. Geophys. Res.: Atmos. 118, 4788–4800.
Toohey, M., Krüger, K., Sigl, M., Stordal, F., Svensen, H., 2016. Climatic and societal impacts of a volcani38c double event at the dawn of the Middle Ages. Clim. Change 136, 401–412.
Toohey, M., Krüger, K., Schmidt, H., Timmreck, C., Sigl, M., Stoffel, M., Wilson, R., 2019. Disproportionately strong climate forcing from extratropical explosive volcanic eruptions. Nat. Geosci. 12, 100–107.
Tupper, A., Textor, C., Herzog, M., Graf, H.-F., Richards, M.S., 2009. Tall clouds from small eruptions: the sensitivity of eruption height and fine ash content to tropospheric instability. Nat. Hazards 51, 375–401.
Turney, C.S., Harkness, D.D., Lowe, J.J., 1997. The use of microtephra horizons to correlate Late-glacial lake sediment successions in Scotland. J. Quat. Sci. 12, 525–531.
Vakhrameeva, P., Portnyagin, M., Ponomareva, V., Abbott, P.M., Repkina, T., Novikova, A., Koutsodendris, A., Pross, J., 2020. Identification of Icelandic tephras from the last two millennia in the White Sea region (Vodoprovodnoe peat bog, northwestern Russia). J. Quat. Sci. 35, 493–504.
van den Bogaard, C., Schminke, H.U., 2002. Linking the North Atlantic to central Europe: a high-resolution Holocene tephrochronological record from northern Germany. J. Quat. Sci. 17, 3–20.
van Dijk, E., Jungclaus, J., Lorenz, S., Timmreck, C., Krüger, K., 2022. Was there a volcanic-induced long-lasting cooling over the Northern Hemisphere in the mid-6th–7th century? Clim. Past 18, 1601–1623.
Vernier, J.P., Fairlie, T.D., Deshler, T., Natarajan, M., Knepp, T., Foster, K., Wienhold, F.G., Bedka, K.M., Thomason, L., Trepte, C., 2016. In situ and space-based observations of the Kelud volcanic plume: the persistence of ash in the lower stratosphere. J. Geophys. Res.: Atmos. 121, 11–104.
Vinther, B.M., Clausen, H.B., Johnsen, S.J., Rasmussen, S.O., Andersen, K.K., Buchardt, S.L., Dahl-Jensen, D., Seierstad, I.K., Siggaard-Andersen, M.-L., Steffensen, J.P., Svensson, A.M., Olsen, J., Heinemeier, J., 2006. A synchronized dating of three Greenland ice cores throughout the Holocene. J. Geophys. Res. 111, D13102.
Vinther, B.M., Clausen, H.B., Johnsen, S.J., Rasmussen, S.O., Steffensen, J.P., Andersen, K.K., Buchardt, S.L., Dahl-Jensen, D., Seierstad, I.K., Svensson, A.M., Siggaard-Andersen, M.-L., Olsen, J., Heinemeier, J., 2008. Reply to comment by J. S. Denton and N. J. G. Pearce on "A synchronized dating of three Greenland ice cores throughout the Holocene". J. Geophys. Res.: Atmospheres 113 (D4), D04304.
Wallace, K., Bursik, M., Kuehn, S., Kurbatov, A., Abbott, P., Bonadonna, C., Cashman, K., Davies, S., Jensen, B., Lane, C., Plunkett, G., Smith, V., Tomlinson, E., Thordarsson, T., Walker, J.D., 2022. Community established best practice recommendations for tephra studies—from collection through analysis. Sci. Data 9, 447.
Wastegård, S., 2002. Early to middle Holocene silicic tephra horizons from the Katla volcanic system, Iceland: new results from the Faroe Islands. J. Quat. Sci. 17, 723–730.
Wastegård, S., Björck, S., Possnert, G., Wohlfarth, B., 1998. Evidence for the occurrence of Vedde Ash in Sweden: radiocarbon and calendar age estimates. J. Quat. Sci. 13, 271–274.
Wastegård, S., Wohlfarth, B., Subetto, D.A., Sapelko, T.V., 2000. Extending the known distribution of the Younger Dryas Vedde Ash into northwestern Russia. J. Quat. Sci. 15, 581–586.
Wastegård, S., Bjorck, S., Grauert, M., Hannon, G.E., 2001. The Mjáuvøtn tephra and other Holocene tephra horizons from the Faroe Islands: a link between the Icelandic source region, the Nordic Seas, and the European continent. Holocene 11, 101–109.
Wastegård, S., Rundgren, M., Schoning, K., Andersson, S., Björck, S., Borgmark, A., Possnert, G., 2008. Age, geochemistry and distribution of the mid-Holocene Hekla-S/Kebister tephra. Holocene 18, 539–549.
Wastegård, S., Johansson, H., Pacheco, J.M., 2020. New major element analyses of proximal tephras from the Azores and suggested correlations with cryptotephras in North-West Europe. J. Quat. Sci. 35, 114–121.
Watson, E.J., Swindles, G.T., Lawson, I.T., Savov, I.P., 2016. Do peatlands or lakes provide the most comprehensive distal tephra records? Quat. Sci. Rev. 139, 110–128.
Watson, E.J., Swindles, G.T., Lawson, I.T., Savov, I.P., Wastegård, S., 2017. The presence of Holocene cryptotephra in Wales and southern England. J. Quat. Sci. 32, 493–500.
Westgate, J.A., Perkins, W.T., Fuge, R., Pearce, N.J.G., Wintle, A.G., 1994. Trace-element analysis of volcanic glass shards by laser ablation inductively coupled plasma mass spectrometry: application to tephrochronological studies. Appl. Geochem. 9, 323–335.
Witham, C.S., Oppenheimer, C., Horwell, C.J., 2005. Volcanic ash-leachates: a review and recommendations for sampling methods. J. Volcanol. Geoth. Res. 141, 299–326.

Wulf, S., Dräger, N., Ott, F., Serb, J., Appelt, O., Guðmundsdóttir, E., van den Bogaard, C., Slowinski, M., Laszkiewicz, M., Brauder, A., 2016. Holocene tephrostratigraphy of varved sediment records from lakes Tiefer See (NE Germany) and Czechowskie (N Poland). J. Quat. Sci. 32, 1–14.

Xu, J., Pan, B., Liu, T., Hajdas, I., Zhao, B., Yu, H., Liu, R., Zhao, P., 2013. Climatic impact of the millennium eruption of Changbaishan volcano in China: new insights from high-precision radiocarbon wiggle-match dating. Geophys. Res. Lett. 40, 54–59.

Yalcin, K., Wake, C.P., Kreutz, K.J., Germani, M.S., Whitlow, S.I., 2006. Ice core evidence for a second volcanic eruption around 1809 in the Northern Hemisphere. Geophys. Res. Lett. 33, L14706.

Yang, Q., Jenkins, S.F., Lerner, G.A., Li, W., Suzuki, T., McLean, D., Derkachev, A.N., Utkin, I.V., Wei, H., Xu, J., Pan, B., 2021. The Millennium Eruption of Changbaishan Tianchi volcano is VEI 6, not 7. Bull. Volcanol. 83, 74.

Zanchettin, D., Khodri, M., Timmreck, C., Toohey, M., Schmidt, A., Gerber, E.P., Hegerl, G., Robock, A., Pausata, F.S., Ball, W.T., Bauer, S.E., Bekki, S., Dhomse, S.S., LeGrande, A.N., Mann, G.W., Marshall, L., Mills, M., Marchand, M., Niemeier, U., Poulain, V., Rozanov, E., Rubino, A., Stenke, A., Tsigaridis, K., Tummon, F., 2016. The Model Intercomparison Project on the climatic response to Volcanic forcing (VolMIP): experimental design and forcing input data for CMIP6. Geosci. Model Dev. (GMD) 9, 2701–2719.

Zdanowicz, C.M., Zielinski, G.A., Germani, M.S., 1999. Mount Mazama eruption: calendrical age verified and atmospheric impact assessed. Geology 27, 621–624.

Zerefos, C.S., Gerogiannis, V.T., Balis, D., Zerefos, S.C., Kazantzidis, A., 2007. Atmospheric effects of volcanic eruptions as seen by famous artists and depicted in their paintings. Atmos. Chem. Phys. 7, 4027–4042.

Zielinski, G.A., 1995. Stratospheric loading and optical depth estimates of explosive volcanism over the last 2100 years derived from the Greenland Ice Sheet Project 2 ice core. J. Geophys. Res.: Atmos. 100 (D10), 20937–20955.

Zielinski, G.A., Mayewski, P.A., Meeker, L.D., Whitlow, S., Twickler, M.S., Morrison, M., Meese, D.A., Gow, A.J., Alley, R.B., 1994. Record of volcanism since 7000 B.C. from GISP2 Greenland ice core and implications for the volcano-climate system. Science 264, 948–952.

Zielinski, G.A., Germani, M.S., Larsen, G., Baillie, M.G.L., Whitlow, S., Twickler, M.S., Taylor, K., 1995. Evidence of the Eldgjá (Iceland) eruption in the GISP2 Greenland ice core: relationship to eruption processes and climate conditions in the tenth century. Holocene 5, 129–140.

Zielinski, G.A., Dibb, J.E., Yang, Q., Mayewski, P.A., Whitlow, S., Twickler, M.S., Germani, M.S., 1997a. Assessment of the record of the 1982 El Chichón eruption as preserved in Greenland snow. J. Geophys. Res. Atmos. 102 (D25), 30031–30045.

Zielinski, G.A., Mayewski, P.A., Meeker, L.D., Grönvold, K., Germani, M.S., Whitlow, S., Twickler, M.S., Taylor, K., 1997b. Volcanic aerosol records and tephrochronology of the Summit, Greenland, ice cores. J. Geophys. Res.: Oceans 102 (C12), 26625–26640.

Zillén, L.M., Wastegård, S., Snowball, I.F., 2002. Calendar year ages of three mid-Holocene tephra layers identified in varved lake sediments in west central Sweden. Quat. Sci. Rev. 21, 1583–1591.